SIMULATION OF TEMPERATURE AND ESTIMATION OF TOOL WEAR IN CRYOGENIC ASSISTED ELECTRICAL DISCHARGE MACHINING PROCESS USING FINITE ELEMENT APPROACH

A Dissertation submitted

in partial fulfillment of the requirements

for the degree of

MASTER OF ENGINEERING

in

CAD/CAM ENGINEERING

by

JASHAN SHARMA

801481011

Under the Supervision of

DR. VINEET SRIVASTAVA

MECHANICAL ENGINEERING DEPARTMENT

THAPAR UNIVERSITY, PATIALA

JUNE, 2016

CERTIFICATE

I hereby declare that the thesis entitled, **"SIMULATION OF TEMPERATURE AND ESTIMATION OF TOOL WEAR IN CRYOGENIC ASSISTED ELECTRICAL DISCHARGE MACHINING PROCESS USING FINITE ELEMENT APPROACH"**, is an authentic record of my study carried out as requirement for the award of degree of **MASTER OF ENGINEERING (CAD/CAM ENGINEERING)** at **THAPAR UNIVERSITY, PATIALA** under the guidance of **DR. VINEET SRIVASTAVA, Assistant Professor, Mechanical Engineering Department, Thapar University, Patiala** during **July 2014 to June 2016**. The matter embodied in this report has not been reported in part or full to any other university or institute for the award of any other degree.

Date: 15/7/2016

Jashan Sharma
Reg. No. 801481011

This is to certify that above declaration made by the student is correct to the best of my knowledge and belief.

15/07/2016

DR. VINEET SRIVASTAVA
Assistant Professor
Mechanical Engineering Department
Thapar University, Patiala- 147004

Countersigned by

Dr. S.K. Mohapatra
Head, Mechanical Engineering Department
Thapar University, Patiala-147004

Dr. S.S Bhatia
Dean of Academic Affair
Thapar University, Patiala-147004

Acknowledgement

I would like to thank all the people who contributed in some way to the work described in this thesis. First and foremost, I thank my thesis supervisor **Dr. Vineet Srivastava, Assistant Professor Mechanical Engineering Department, Thapar University, Patiala** for his guidance, support, inspiring suggestion and the development of thesis at every step. He took keen interest in my report and helped me to access facilities of Mechanical Engineering Department laboratories.

I would also like to thank **Dr. S.K. Mohapatra, Head & Senior Professor, Mechanical Engineering Department, Thapar University, Patiala** for providing facilities for completion of the work.

A special thanks to my friend Bikramjeet Singh for his help and support during thesis work.

In the end, I wish to express my deep sense of gratitude to my family, for supporting and encouraging me at every step of my work. It is the power of their blessings, which has given me the courage, confidence and zeal for hard work.

Jashan Sharma

ABSTRACT

EDM is a process that is based on removing material from a conducting workpiece by means of a series of repeated electrical discharges between tool electrode (cathode) and the workpiece (anode) in the presence of a dielectric fluid. Despite all the advantages, the EDM process is not free from drawbacks. One of the major drawbacks is the high rate of electrode wear. Cryogenic assisted EDM is a hybrid process which utilizes the cooling properties of liquid nitrogen to reduce the temperature of the electrode so as to reduce electrode wear. Experimentally it has been proved that cryogenic cooling in EDM has reduced tool wear. However there exist no information regarding the size and dimensions of the crater formed in cryogenic assisted EDM process. Further the effect of cooling on temperature is also not available. Therefore in this present work, an effort has been made to study the effect of cryogenic cooling on temperature and the estimation of the size and dimensions of the crater on tool in cryogenic assisted EDM process. Temperature simulations have been performed for both conventional EDM process and cryogenic assisted EDM process to understand the temperature distribution along the length and diametrical axis of the tool electrode. The finite element approach has been employed to predict the temperature profile on the tool electrode under various operating conditions. Further in the work, an estimation of the radius and depth of crater has been performed in order to predict the tool electrode wear rate for both conventional EDM and cryogenic assisted EDM. An algorithm has been developed that reads and plots the temperature distribution along x and z axis of the surface of the tool giving radius and depth of crater. Further, using the radius and depth of crater, volume of melted portion of tool electrode and electrode wear rate for both conventional EDM and cryogenic assisted EDM have been calculated. It has been observed that cryogenic assisted EDM has lower tool temperature as compared to conventional EDM process. It has also been observed that the radius and depth of crater is smaller in cryogenic assisted EDM as compared to conventional EDM. Further it has been established that the tool electrode wear is more in conventional EDM process as compared to cryogenic assisted EDM process.

Keywords: Conventional EDM, Cryogenic assisted EDM, Electrode wear rate, Temperature distribution, Radius of crater, Depth of crater

CONTENTS

LIST OF FIGURES

LIST OF TABLES

NOMENCLATURE

EDM	Electrical Discharge Machining
CEDM	Cryogenic assisted EDM
EDM	Finite element analysis
EWR	Electrode wear rate
FEA	Finite element analysis
Fa	Fraction of the total heat that goes into the anode
Fc	Fraction of the total heat that goes into the cathode
I	Discharge current
MRR	Material removal rate
q(r)	Heat flux q(r) entering the tool
Rp	Spark radius
Ton	Pulse on-time
Toff	Pulse off-time
V	Discharge voltage
V_t	Volume of melted portion of tool electrode

CHAPTER 1

INTRODUCTION

1.1 BACKGROUND

The recent advancement in various technological field demands the development and use of new materials, which can sustain external loads at extremely high temperatures and corrosive environments. The use of thermoelectric source of energy in developing the nontraditional techniques has greatly helped in achieving an economic machining of extremely low machinability materials and jobs with complex geometries. There are many processes in which metal removal is based on thermal principles and Electrical Discharge Machining (EDM) is one of them.

The general features of an EDM machine are given in figure 1.1. Fundamentally, electro sparking method of metal working involves electric erosion effect which connotes the breakdown of electrode material accompanying any form of electric discharge. A necessary condition for producing a discharge is the ionization of the dielectric that is splitting up of dielectric molecules into ions and electrons.

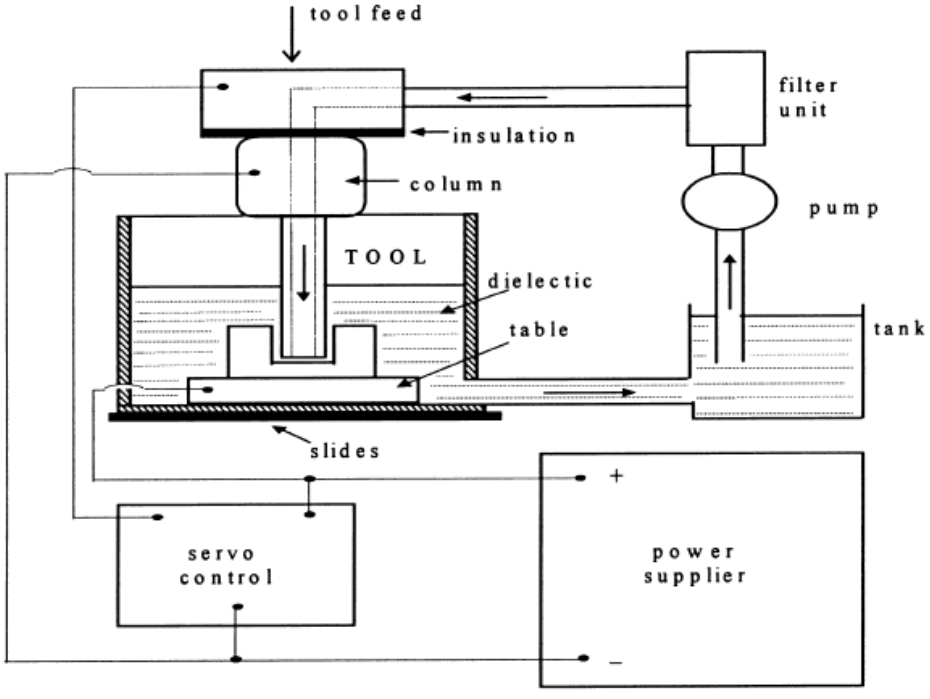

Figure 1.1: General features of EDM.[1]

There is a discharge between tool cathode and work anode through a gaseous or a liquid medium. As suitable voltage is applied across the electrodes, the potential intensity of the electric field between them builds up until at some predetermined

value, the individual electrons break loose from the surface of cathode and are impelled towards the anode under the influence of field forces. While moving in the inter-electrode gap, the electrons collide with dielectric molecules, detaching electrons from them and causing ionization. At some time the ionization becomes such that a narrow channel of continuous conductivity is formed. This results in a considerable flow of electrons along the channel to anode, resulting in momentary current impulse or discharge. The liberation of energy accompanied the discharge leads to the generation of very high temperature causing fusion or partial vaporization of the metal and the dielectric at the point of discharge. The metal is dispersed into space surrounding the electrons by the explosive pressure of the gaseous products in the discharge. This results in formation of tiny craters at the point of discharge. Less metal is eroded from the cathode as compared to anode [2, 3].

EDM does not make direct contact between the electrode and the workpiece whereby it can eliminate mechanical stresses, chatter and vibration problems during machining. Although this does not mean that induced stresses and metallurgical effects on the workpiece are necessarily absent [4]. EDM has been widely accepted by the metal cutting industries for the machining of heat treated tool steel, high strength alloys and carbides. EDM is also capable of machining ultra-hard tool materials such as polycrystalline diamond, CVD diamond, PVD coated cemented carbide and conducting ceramics. The development of different modern composite materials in the last decade has led to an expansion of EDM applications in the manufacturing of mould, die, automotive, aerospace and surgical components. The volume of material removed per discharge is typically in the range of 10^{-6}–10^{-4} mm3 and the material removal rate (MRR) is usually between 2 and 400 mm^3/min. The surface finish produced by the EDM process consists of a multitude of small craters randomly distributed all over the machined face. Typical surface finish range is about 1.6 to 3.2 μm, although there are claims of 0.05 to 0.1 μm also. Normal tolerances of about ± 25 μm are obtainable by proper selection of process variables [3, 4]. The two most widely used types of EDM are die sinking EDM and wire EDM (WEDM). Die sinking EDM is widely used in the mold making industries. The advent of computer numerical control (CNC) in EDM brought tremendous advances in improving the efficiency of the machining operation [5, 6].

The mechanism of material removal is very complex in EDM process and no single theory can explain it in a comprehensive manner. The material removal in

EDM is considered to be prominently governed by three different erosion theories namely high temperature theory, static field theory and high pressure theory [7]. However, the high temperature theory is widely acceptable which can take care to explain the major portion of the stock removal phenomenon.

EDM characteristics have been investigated over the last five decades. A broad look at the literature reveals that EDM of steels has received maximum attention. EDM machining tool manufacturers have also been providing machining data for steels based on their in house experimentation. Such data base is based on the quantitative and qualitative relationship between the technological parameters like erosion rate and surface integrity and input variables like work and tool materials properties and machining parameters like current, pulse duration, duty cycle, etc. [8].

1.2 PROBLEM AREA OF EDM

Despite having all the advantages, the EDM process is not free from drawbacks. One of the major drawbacks is the slow rate of material removal. Other drawbacks include surface and subsurface damage, creation of thin and brittle heat-affected zone and high rate of electrode wear. In light of these defects, researchers have developed new techniques using ultrasonic [9], gas based method [10], dry EDM [11], EDM with powder additives [12], EDM in water [13], cryogenic assisted EDM [14] and ultrasonic assisted cryogenically cooled EDM process [15] where they tried to overcome the above limitations.

1.3 CRYOGENIC ASSISTED EDM PROCESS

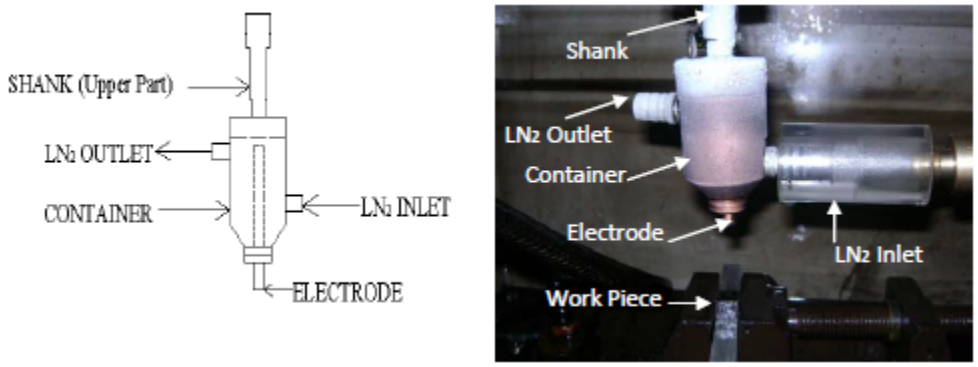

Figure 1.2: (a) The schematic diagram of electrode attachment (b) The electrode setup mounted on the EDM machine [16]

The setup for cryogenic assisted EDM process has been shown in figure 1.2. An attachment has been designed and developed to use liquid nitrogen cooled electrode for EDM process. The attachment is mounted on the EDM machine spindle

using a hollow shank and it has the feed motion (Z direction tool movement) from the Z-NC machine control. The cryogenic Dewar has been used for controlled supply of liquid nitrogen to the electrode cooling attachment.Cryogenic assisted EDM is an hybrid process which utilizes the cooling properties of liquid nitrogen to reduce the temperature of the electrode so as to reduce electrode wear.

As highlighted above, the high temperature theory is widely acceptable which can take care to explain the major portion of the stock removal phenomenon in EDM. This theory states that material removal is mainly due to melting and evaporation. Cryogenic cooling in the present experimental work has reduced MRR and tool wear which again supports the applicability of high temperature theory in EDM. It can also be concluded that the mechanism of sparking and material removal does not change, but due to cryogenic cooling of the tool electrode, the temperature of the electrode decreases. Due to this reduction in temperature, more time is taken up for ignition of the discharge to be initiated as compared to EDM. As the ignition of the discharge starts, high amount of heat is generated in the ionized zone. However some amount of heat generated in ionized zone is utilized to maintain the temperature of the electrode at elevated level. As a result, the effective heat that is transferred to the work piece is reduced resulting smaller formation of the crater. This results in reduction of MRR as compared to EDM [16].

1.4 FINITE ELEMENT ANALYSIS

The finite element analysis is a numerical technique for finding approximate solutions of partial differential equations. Mathematical model of a phenomena or processes are developed using assumption concerning how the physical process or phenomena works and laws governing the process and they are generally characterized by very complex differential and/or integral equation applicable on geometrically complicated domains. Numerical methods of analysis provide alternative means of finding solution of mathematical model of physical problem. Numerical methods typically transform differential equation (which is applicable to whole model domain) to a set of algebraic equations (which are applicable to discrete model domain). The Finite Element Method is one of the numerical methods but is more general and powerful in application to the real world problems that involve the complicated physics, geometry and boundary conditions. In the FEM, a given domain is considered as a collection of subdomains which are called as finite elements and

over each subdomain the governing differential equation is approximated by any variational methods [17]. Steps involved in the finite element method of a typical problem are:

a) Discretization of a given domain into subdomains of preselected element type.
b) Choose the approximate solution and derive element level governing equation for all types of element in mesh.
c) Assemble the element level governing equation to obtain the equation of the whole domain.
d) Impose the initial and boundary condition of the problem.
e) Solve of the assembled equation to obtain the unknown variable.
f) Post-processing of the results.

Based on the studies conducted it was found that Finite element analysis is one of the most dominantly used tools for analysis of mathematical model of EDM. Mathematical modeling of EDM is based on heat transfer techniques so they are referred as thermal models [18]. The finite element solution of a problem provides us the approximate behavior of the model under the defined boundary conditions, but the accuracy of the results of the analysis depends on the accuracy of the input.

1.5 MOTIVATION

It has been observed that excessive heat and subsequently wear of the tool are the most important factors affecting performance and productivity of machining operations. In machining operations, wear of the tool is an unavoidable phenomenon and it eventually leads to the failure of the tool. It has been observed that the conventional cooling methods are not effective. They eventually deteriorate the working environment by producing harmful gasses and smokes. The rate of electrode wear is significant in the case of a small diameter electrode and it is particularly higher for the difficult to machine materials like ceramic composites. The reduction in tool wear is important to improve the productivity of EDM. In cryogenically cooled EDM process, it has been reported that cryogenic cooling of the electrode reduces the tool wear and the temperature of copper electrode [16]. In view of these factors, the present work investigates the effect of temperature on the wear of copper electrode in cryogenic assisted EDM process.

1.6 ORGANISATION OF THE THESIS

The research work has been organized as follows:

Chapter 1 presents an introduction to EDM process. It provides overview of different theories of material removal, integration of other technologies with EDM, advantages and limitations of EDM process. it provides a background of cryogenic assisted EDM process and finite element analysis. This chapter also gives an overview of the motivation and thesis organization.

Chapter 2 provides a critical review of literature on cryogenic assisted EDM process and modelling of EDM process. Research gaps have been identified, objectives have been framed and methodology followed for fulfilling the objectives presented.

Chapter 2 provides a critical review of literature on cryogenic assisted EDM process and modelling of EDM process. Research gaps have been identified, objectives have been framed and methodology followed for fulfilling the objectives presented.

Chapter 3 is focused on the temperature of the electrode. Spark radius and heat flux generated have been calculated for different cases in cryogenic assisted EDM process and EDM process. Further temperature simulations have been performed for both the processes to understand the temperature distribution along the length of the electrode. An assessment of the variation of temperature along the diameter of the electrode tip has also been studied.

Chapter 4 is dedicated to the size and shape of the crater, material removed from the tool electrode and electrode wear rate of the tool. Radius and depth of crater generated have been calculated for different cases in cryogenic assisted EDM process and EDM process. The shape of the crater has been analyzed. Further, the volume of melted electrode from the tool has been calculated. An assessment on the variation of electrode wear rate of tool has also been studied for both cryogenic assisted EDM process and EDM process.

Chapter 5 summarizes the major findings of the research work carried out and the directions of the future research have been highlighted.

CHAPTER 2

LITERATURE REVIEW

2.1 INTRODUCTION

EDM being a thermal process is unavoidably accompanied with high rates of electrode wear which requires more number of electrodes to be fabricated for a job. In EDM, the cost of machining also increases as the manufacturing of electrodes accounts for over 70% of the total machining cost [19]. The rapid electrode wear could be reduced by an efficient cooling strategy as EDM being a thermally dominated process. Cryogenic cooling and environmental friendliness have been investigated and established to control cutting zone temperature in machining of steels and also titanium alloys with substantial technological benefits. Few researchers have investigated influence of cryogenic cooling using liquid nitrogen in EDM. Research efforts carried out in the past to investigate experimentally the influence of cryogenic cooling using liquid nitrogen on tool electrode wear has been discussed in this chapter.

The literature review presented in this section is based on current research trend in modelling of tool wear in electrical discharge machining process. The present work is concerned with mathematical modelling of EDM process. In this context, some of the related research contributions made in the past by researchers have also been discussed in this chapter.

2.2 CRYOGENIC ASSISTED EDM PROCESS

Abdul kareem et al. [14, 20] studied the cooling effect of copper electrode on the die-sinking of electrical discharge machining of titanium alloy (Ti-6Al-4V). Effect of cooling on electrode wear (EW), material removal rate (MRR) and surface roughness (Ra) of the workpiece has been investigated. It has been reported that it was possible to reduce electrode wear ratio up to 27% by electrode cooling while MRR and Ra were improved by 18% and 8% respectively.

Srivastava and Pandey [21, 22] studied the cooling effect on copper electrode while electrical discharge machining (EDM) M2 grade high speed steel workpiece. Electrode wear ratio (EWR) and surface roughness (SR) were the two responses observed. Discharge current, pulse on time, duty cycle, and gap voltage were the controllable process parameters. It was found that EWR reduced up to 20% by cryogenic cooling of electrode. With electrode cooling, SR was also found to have

been reduced after machining. EWR and SR have been found to be lower in cryogenic assisted EDM as compared to EDM for the same set of process parameters. The shape of the electrode was measured, and it was found that the shape retention was better in cryogenic assisted EDM as compared to EDM. It has been further concluded that the mechanism of sparking and material removal did not change, but due to cryogenic cooling of the electrode, the temperature of the electrode decreased, resulting in smaller formation of the crater. This resulted in reduction of MRR as compared to EDM.

2.3 MODELLING OF EDM PROCESS

EDM process is influenced by many input factors like discharge current, gap voltage, discharge duration, duty cycle etc. Various techniques like dimensional analysis, artificial neural network and mathematical modeling are used to predict the output of the process mainly the material removal rate, tool wear rate and surface finish.

Dibitonto et al. [23] developed a cathode erosion model for EDM process considering point heat-source and assuming that there is one spark per pulse. In this model, it has been concluded that 18% of the total power supplied is transferred to cathode over a wide range of currents. This fraction of power is independent of discharge current and pulse time however it may change when either electrode or dielectric fluid is replaced by different materials. Here an effective value of thermo physical properties of material is considered over temperature range from room temperature to melting point.

Patel et al. [24] developed an anode erosion model considering expanding circle heat source. This model assumes single spark per pulse and the plasma radius continuously grows with time. it has been concluded that 8% of total power is transferred to the anode. The supplied power produces Gaussian-distributed heat flux on the surface of the anode. The model is capable of showing, the rapid melting of the anode as well as the subsequent resolidification of the material for longer durations of time.

Eubank et al. [25] developed a model for the spark created by electrical discharge in a liquid medium. The model consists of differential equations from fluid dynamics, energy balance and radiation. The spark radius near the cathode is much smaller than that near the anode but the shape of spark is assumed to be cylindrical.

Numerical solution of the model provides plasma radius, temperature, pressure, and mass as a function of pulse time for fixed current, electrode gap, and constant power fraction (74%) that remains in the plasma.

Singh and Ghosh [26] developed a model which explains the removal of material due to electrostatic forces acting on the surface of the electrode that creates the craters. They proposed thermo-electric model for calculating the electrostatic force on the surface of the cathode and the stress distribution inside the metal during the discharge. The model was valid for short pulses. They proposed that the electrostatic forces are the major cause of metal removal for short pulses. For long pulses, the dominant phenomenon was melting.

Marafona and Chousal [27] developed a thermal–electrical model for sparks generated by electrical discharge in a liquid medium. The joule heating effect is considered as the main source of thermal energy to increase the discharge channel temperature and melt both the electrodes. This model is used to estimate the surface roughness, material removed from cathode and anode and the maximum temperature in the discharge channel.

Salah et. al [28] presented numerical results explaining the temperature distribution for EDM process. From the thermal results, the material removal rate and the total roughness were deduced and compared with experimental observations. It was shown that taking into account the temperature variation of conductivity is of crucial importance and gives the better correlations with experimental data.

Jilani and Pandey [29] presented an analytical model for the computation of metal erosion by a single spark in electrical discharge machining process. This analytical model assumed disc shape heat source and used to compute the rate of metal removal and electrode wear ratio in situations where the current pulse is non-rectangular. The thermal model for EDM based on plasma channel growth considerations yields accurate results. The effect of plasma channel growth on metal removal was examined and good correlation was found between theoretical and experimental results.

Joshi and Pande [30] reported the development of a thermo-physical model for die-sinking EDM process using finite element method. Numerical analysis of the single spark operation of EDM process has been carried out considering the two-dimensional axi-symmetric process continuum. This analysis is based on assumptions such as Gaussian distribution of heat flux, spark radius equation based on discharge

current and discharge duration, to predict the shape of crater cavity and the material removal rate. Developed model is used for parametric studies to analyse the effect of discharge current, discharge duration, discharge voltage and duty cycle on the process performance.

2.4 RESEARCH GAP

From the literature survey of modelling of EDM process, it can be concluded that erosion mechanism is basically a thermal process. Thermal models are developed for erosion by single spark. Based on the available literature, it can be concluded that most of the works related to cryogenic assisted EDM are experimental. It has been reported in the literature that due to cryogenic cooling of the electrode, the temperature of the electrode decreases, resulting in formation of smaller crater. However there is no literature available which can theoretically or experimentally validate the above assertion.

2.5 RESEARCH OBJECTIVE

The objectives of this work are

- To determine and compare the temperature distribution along the length and along the diameter of the tool electrode in cryogenic assisted EDM process and EDM process using finite element simulation.
- Thermal analysis of cryogenic assisted EDM process to predict the depth and radius of crater on the tool electrode and estimation of electrode wear rate for different operating conditions and its comparison with EDM process.

2.6 METHODOLOGY

- Identify the correlation to predict the spark radius for the EDM process.
- Identify the correlation to predict the heat flux for electrode and workpiece for the EDM process.
- Suitable assumptions were made to determine and compare the temperature distribution along the length and along the diameter of the tool electrode.
- Develop a 2D axi-symmetric thermal finite element single spark model to determine and compare the temperature distribution along the length and along the diameter of the tool electrode in cryogenic assisted EDM process and EDM process.

- Develop a 3D model of tool electrode and apply heat flux by discretizing it in accordance with Gaussian distribution.
- Develop an algorithm which gives the plots between the temperature and radial distance from spark centre.
- Estimate the depth and radius of crater on the tool electrode for cryogenic assisted EDM process and EDM process.
- Calculate the electrode wear rate for different operating conditions of cryogenic assisted EDM process and EDM process.
- Conclusions

CHAPTER 3

TEMPERATURE DISTRIBUTION USING FINITE ELEMENT SIMULATION IN CRYOGENIC ASSISTED EDM PROCESS AND EDM PROCESS.

3.1 INTRODUCTION

The multi-variety and small batch production has become a trend to meet the consumers' aspirations which have shortened product life cycle. This needs to reduce the period of the product design and fabrication. Therefore, efficiency, effectiveness, and reliability become buzzwords of manufacturing process development. The rate of electrode wear is significant in the case of a small diameter electrode and it is particularly higher for the difficult to machine material like ceramic composites. The reduction in tool wear is important to improve the efficiency of EDM. The rapid electrode wear can be reduced by an efficient cooling strategy. An attempt of liquid nitrogen cooled electrode has shown to control electrode wear. The normal boiling temperature of liquid nitrogen is –196°C. In the present chapter, the finite element analysis has been carried out to obtain the temperature profile at various points on the tool electrode. The analysis has been performed across the diameter and along the length of the electrode to gain better understanding of the temperature distribution. A comparative performance analysis of liquid nitrogen cooled electrode EDM and EDM has been attempted. The present investigation provides a valuable source of reference for the use of small area copper electrodes in EDM process.

3.2 FINITE ELEMENT ANALYSIS

The FE analysis is carried out to find out the temperature profile at various points on the tool electrode. The FEA is accomplished using the ANSYS 15.0 package. The main aim of the FE analysis is to study the effect of cryogenic on the temperature distribution on the tool electrode. To simplify the complex analysis, certain assumptions have been made based on the previous research attempt on electro-thermal modeling of anode in EDM [24, 31] and are given by

- The nature of tool material is homogeneous and isotropic.
- The material properties of tool are temperature dependent.
- The model is developed for a single spark.
- Heat Transfer to the electrodes is through conduction.

- Only a fraction of discharge energy is able to reach to the electrode.
- The work domain considered is axisymmetric about r-z plane.
- Heat flux is assumed to be Gaussian-distributed.
- Temperature analysis is considered to be of steady state.
- The energy used electrode wear is generated by voltage and current during pulse on time.
- The diameter of the electrode is very small.

3.3 GOVERNING EQUATION

Fourier heat conduction equation is taken as the governing equation for the thermal analysis of EDM process [31]. All discharges can be considered to be identical, so the analysis has been carried out for a single spark operation.

$$\frac{\partial^2 T}{\partial r^2} + \frac{1}{r}\left(\frac{\partial T}{\partial r}\right) + \frac{\partial^2 T}{\partial z^2} = \frac{\rho C_p}{K}\left(\frac{\partial T}{\partial t}\right) \ldots\ldots\ldots\ldots\ldots\ldots\ldots\ldots\ldots\ldots\ldots\ldots (3.1)$$

Where r and z are the cylindrical coordinates of work space; T is temperature; K is thermal conductivity; ρ is density; C_p is specific heat capacity of material and t is time.

3.4 BOUNDARY CONDITIONS

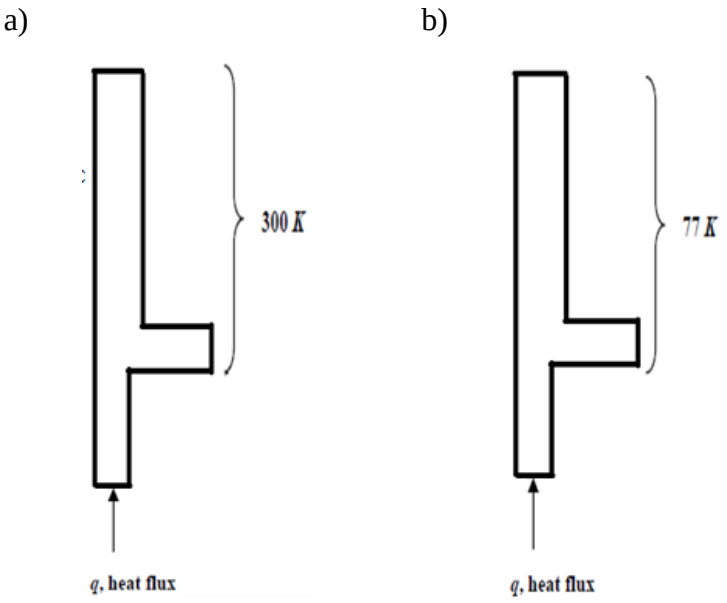

Figure 3.1: Boundary conditions for a) conventional EDM process b) cryogenic assisted EDM process.

Boundary conditions are selected at three locations on the electrode. The boundary conditions include temperature at known locations. For finite element analysis of EDM using liquid nitrogen cooled small diameter electrode, the temperature at the junction of liquid nitrogen with the electrode is taken as 77 K. The

temperature of the electrode surface which is in contact with the dielectric is taken to be equal to room temperature. For the finite element analysis of EDM using a small diameter electrode without liquid nitrogen, the temperature at the top of the electrode is also taken to be equal to room temperature that is 300 K. The boundary conditions used in FEM analysis during cryogenic assisted EDM process and EDM process is shown in Fig. 3.1.

3.5 RADIUS OF SPARK

The spark radius which indicates the size of heat flux on the workpiece surface is an important factor in the modeling of the EDM process. Some researchers considered the spark radius is time dependent, others considered the spark radius is time and current dependent.

Eubank et al. [25] considered variable mass cylindrical plasma model which shows the dependence of plasma radius on discharge duration. This methodology has been adopted to calculate spark radius at cathode and anode.

$$R_p = 0.788 \times (T_{on})^{0.75} \quad \ldots\ldots\ldots\ldots\ldots\ldots\ldots\ldots\ldots\ldots\ldots\ldots\ldots (3.2)$$

Where Ton indicates the spark on time and Rp is spark radius.

3.6 HEAT OF A SPARK

In this present work, to approximate the heat from the plasma, the Gaussian heat input model has been used. As Dibitonto et al. [23] mentioned, although the point heat source approximation or uniformly distributed heat flux model is acceptable for analytical work, the Gaussian model still remains the best approximation of the heat input. The Gaussian model has two factors, the fraction of heat applied to the workpiece and the radius of the area heated by the plasma.

The heat flux q(r) entering the workpiece due to EDM spark [31] is represented by equation 3.3.

$$q(r) = q_0 e^{\left\{-4.5\left(\frac{r}{R_p}\right)^2\right\}} \quad \ldots\ldots\ldots\ldots\ldots\ldots\ldots\ldots\ldots\ldots\ldots\ldots\ldots (3.3)$$

Where ‘r’ is the radial distance at any point from the centre of the spark and Rp is the spark radius or plasma radius. The maximum heat flux q_0 can be calculated by equation 3.4.

$$q_0 = \frac{4.56 \times F_c \times V \times I}{\pi R_p^2} \quad \ldots\ldots\ldots\ldots\ldots\ldots\ldots\ldots\ldots\ldots\ldots\ldots\ldots (3.4)$$

Where Fc is the fraction of total energy going to the cathode, V is discharge voltage (V), I is current (A) and Rp (μm) is spark radius at the work surface. In present

analysis discharge voltage is taken as 25V. Table 3.1 shows the spark radius and maximum heat flux supplied to tool electrode for different discharge current and discharge duration.

Table 3.1: Spark radius and Maximum heat flux for different operating conditions [16,32]

S.No.	Pulse on time (µs)	Discharge current (A)	Spark radius (µm)	Maximum heat flux on tool (w/mm^2)
1	32	10	10.602022	258397.1908
2	56	20	16.13122087	223234.1898
3	100	5	24.91874796	23387.44395
4	100	25	24.91874796	116937.2197
5	180	36	38.72403432	69727.88598
6	200	4	41.90817167	6614.968084
7	24	8.5	8.544460546	338154.2253
8	240	44	48.04903267	55353.94389
9	300	5	56.80246183	4500.915686
10	300	7	56.80246183	6301.28196
11	300	3	56.80246183	2700.549412
12	400	6	70.48086265	3508.116592
13	400	4	70.48086265	2338.744395
14	420	58	73.10771082	31518.59235
15	500	5	83.32085556	2091.836579

3.7 SIMULATIONS OF TEMPERATURE ALONG THE LENGTH OF ELECTRODE

The governing equation with boundary conditions as mentioned above is solved by FEM to estimate the temperature distribution with the heat flux at the spark

location and the discharge duration as the total time step. The analysis of the model was carried out using ANSYS 15.0 software.

An axisymmetric 2-dimensional model was created for thermal analysis. The domain is discretised by unstructured mesh with TET element. Considering the variation of thermo-physical properties over a temperature range from ambient to melting point, effective values are used for density, thermal conductivity and specific heat. The effective values used were values averaged over the entire temperature range rather than a single value at average temperature as used by Dibitonto et al. [23]. Convergence condition was tested by increasing the number of elements in the mesh and is given in table 3.2. It was observed from the table that the variation of temperature was very minimal when we increased the number of elements from 2228 onwards. Hence, based on this study, a converged mesh of 2228 elements has been considered. This study was performed for both EDM process and cryogenic assisted EDM process.

Table 3.2: Test for convergence of temperature

S. No	**No. of elements**	**Max. Temperature (°C)**
1	152	903.48
2	2228	910.84
3	8994	911.00
4	31258	911.30

The maximum temperature attained at the tool tip has been given in table 3.3, which clearly shows that the temperature of the electrode tip in cryogenic assisted EDM process is less that the electrode temperature in EDM process for the same process conditions. The simulations for the cases mentioned in table 3.1 have been presented in table 3.4.

Table 3.3: Maximum temperature at the electrode tip for conventional EDM process and cryogenic assisted EDM process.

S.No.	CONVENTIONAL EDM PROCESS (°C)	CRYOGENIC ASSISTED EDM PROCESS (°C)
1	3911.2	3688.4
2	3134.4	2911.4
3	1969.0	1746.0
4	2746.0	2523.0
5	2357.5	2134.5
6	1192.0	959.0
7	3678.2	3455.2
8	2202.2	1979.2
9	1580.7	1357.7
10	1813.7	1590.7
11	959.0	736.0
12	1425.3	1202.3
13	1736.0	1513.0
14	2901.2	2678.3
15	2512.9	2289.9

Table 3.4: Temperature simulation results for conventional EDM process and cryogenic assisted EDM process.

S.No.	CONVENTIONAL EDM PROCESS	CRYOGENIC ASSISTED EDM PROCESS
1	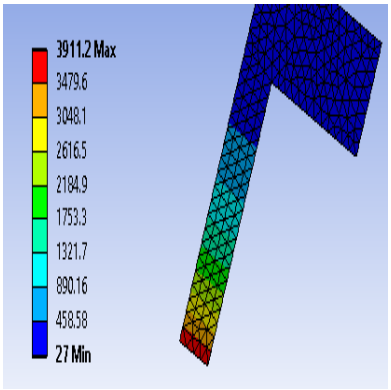	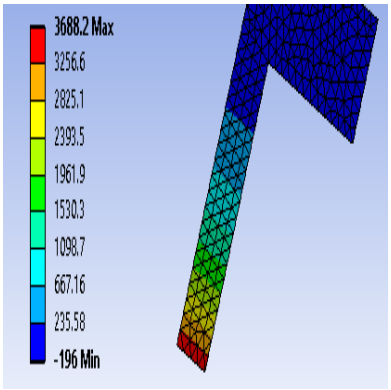
2	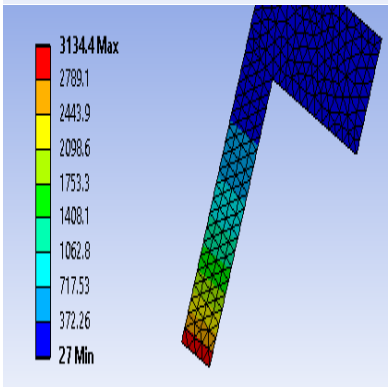	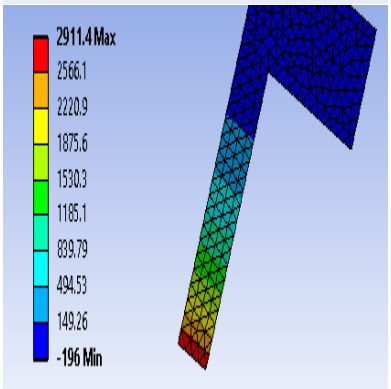
3	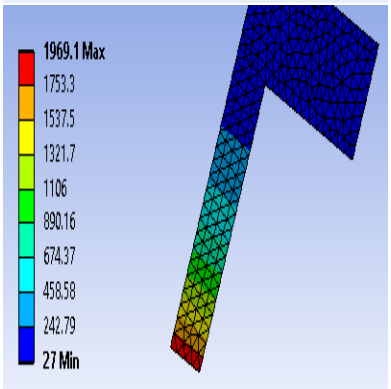	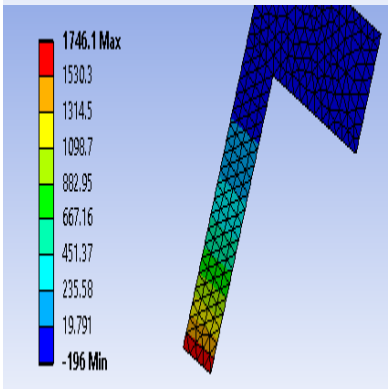
4	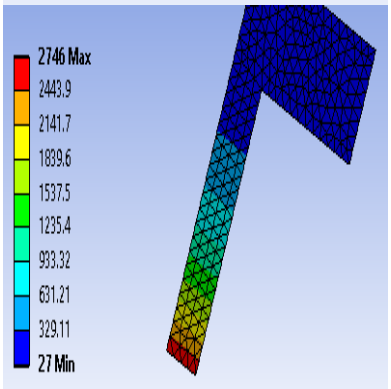	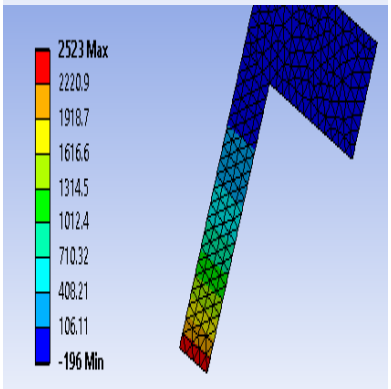

S.No.	CONVENTIONAL EDM PROCESS	CRYOGENIC ASSISTED EDM PROCESS
5	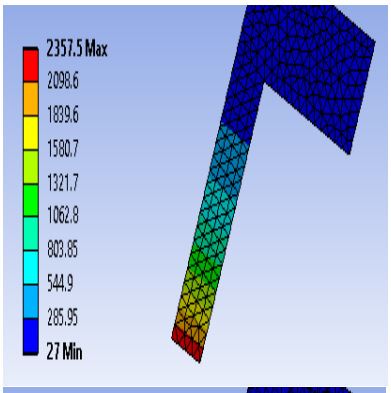	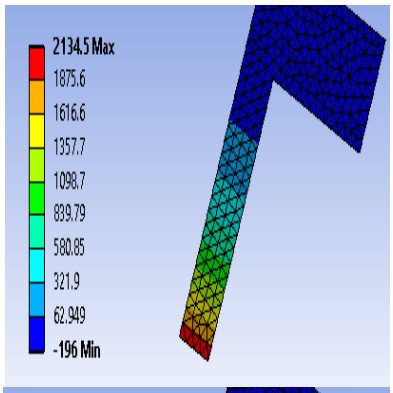
6	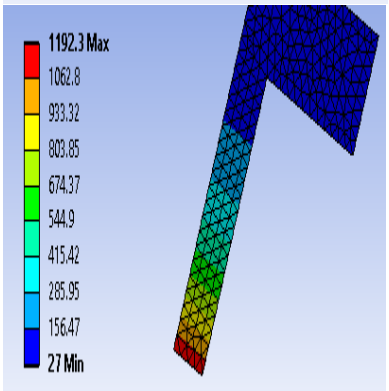	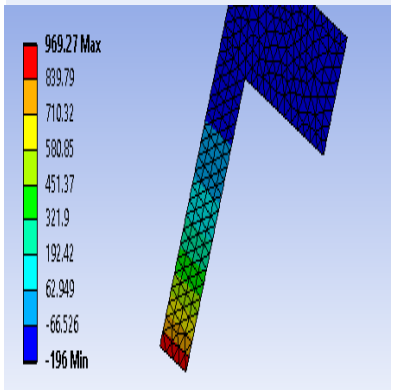
7	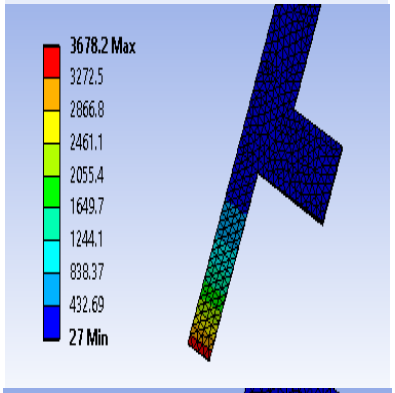	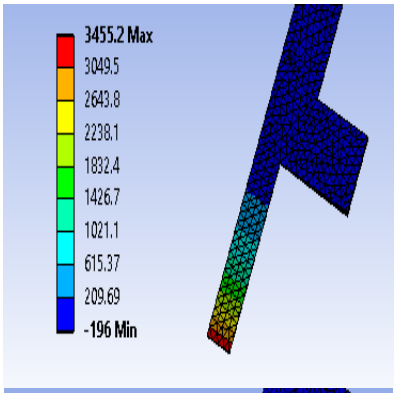
8	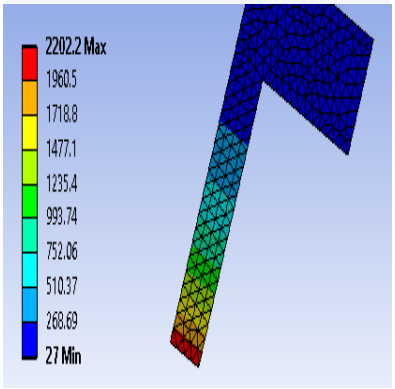	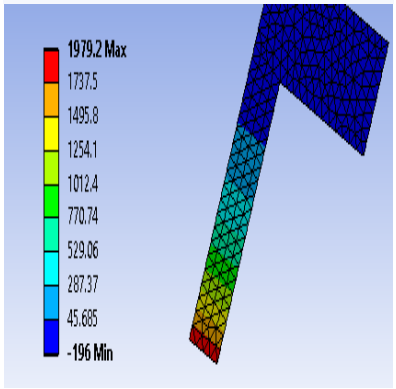

S.No.	CONVENTIONAL EDM PROCESS	CRYOGENIC ASSISTED EDM PROCESS
9	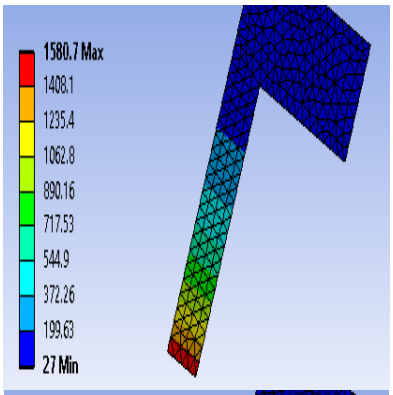	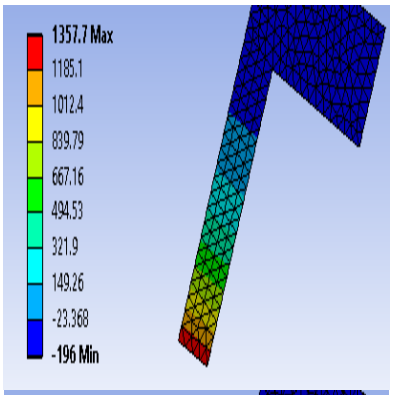
10	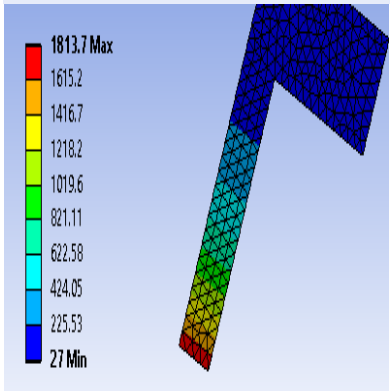	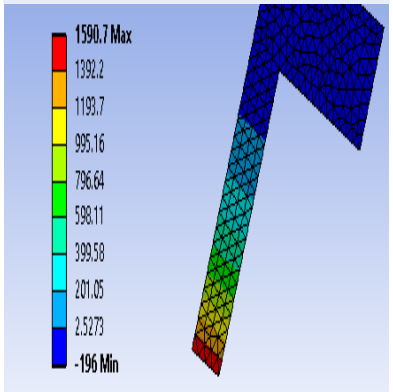
11	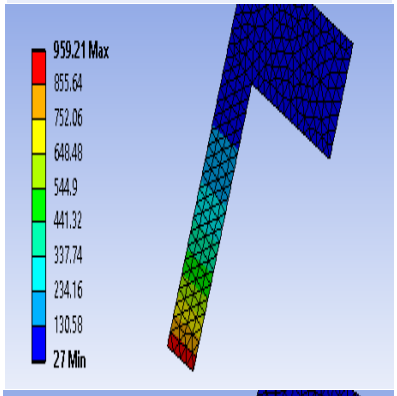	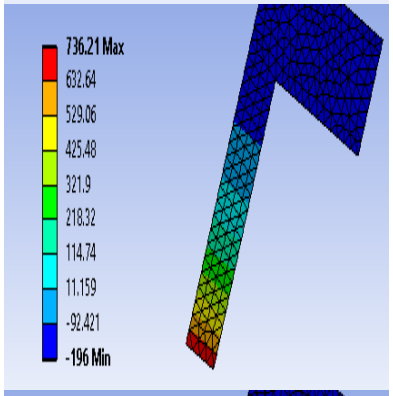
12	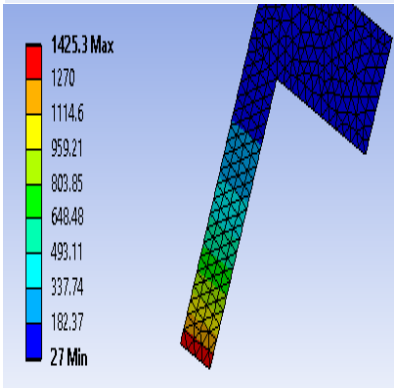	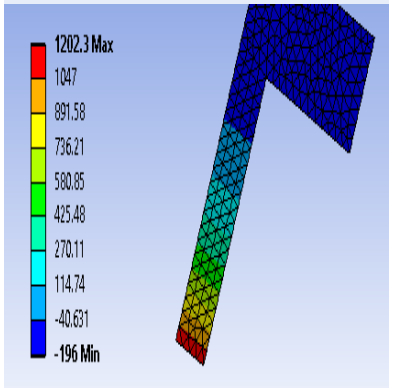

S.No.	CONVENTIONAL EDM PROCESS	CRYOGENIC ASSISTED EDM PROCESS
13	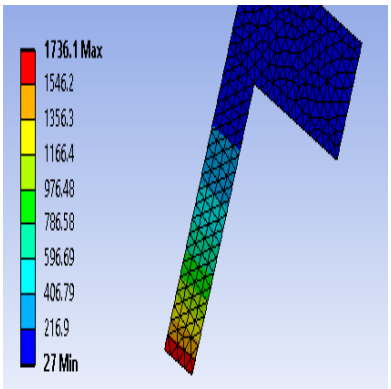	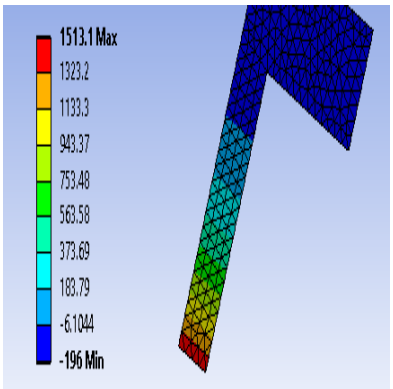
14	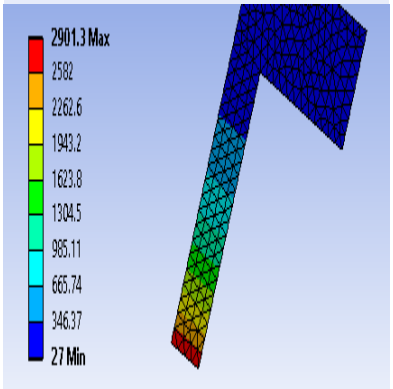	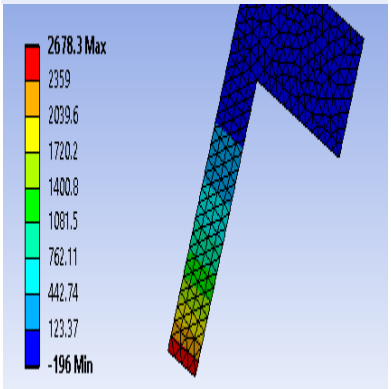
15	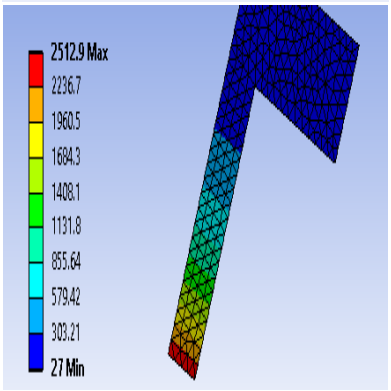	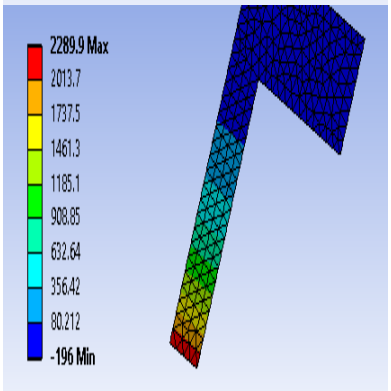

3.8 VARIATION OF TEMPERATURE ALONG THE DIAMETER OF ELECTRODE

The temperature distribution along the diameter of the tool electrode at the surface of the electrode has also been obtained for both EDM process and cryogenic assisted EDM process. Here, the known input heat flux was discretised in 10 parts on the geometry of circular cross-section. The spark radius obtained by the equation 3.2 was also divided into 10 equal sections. Now the flux distribution in each segment was calculated by equation 3.3 and applied accordingly as shown in figure 3.2.

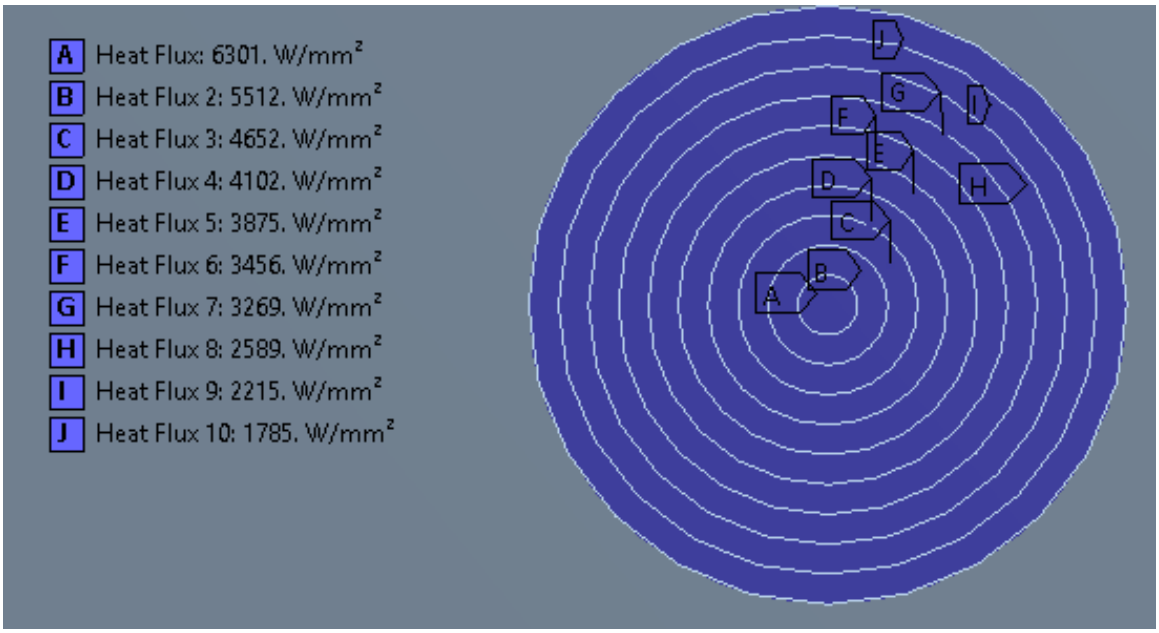

Figure 3.2: Different Heat Fluxes applied on different locations following Gaussian distribution

Table 3.5: Temperature at different locations along the diametrical axis for conventional EDM process and cryogenic assisted EDM process.

S.No.	CONVENTIONAL EDM PROCESS (°C)		CRYOGENIC ASSISTED EDM PROCESS (°C)	
	Temperature at r = 0	Temperature at r = R	Temperature at r = 0	Temperature at r = R
1	19230	2160	19005	1947
2	24919	2792	24696	2586
3	3884	679	3661	493
4	13075	1476	12852	1263
5	5930	895	5710	658
6	2004	246	1782	157
7	2558	313	2336	115
8	5785	735	5558	601
9	4075	476	3852	273
10	6232	726	6100	536
11	1372	176	1149	102
12	2966	353	2743	150
13	2736	388	2513	223
14	3610	642	3405	419
15	5448	629	5225	426

The simulations were performed according to the pre-decided boundary conditions. The details of each node, containing information of the nodal coordinates

and the temperature derived from the simulation, was transferred to an excel file. This file was sorted for the temperature along the x-axis. Now all the temperature along x-axis which have y and z coordinates as zero (0) were selected and transferred to another file. From this file, a plot was obtained depicting the temperature distribution along the diametrical axis. Table 3.5 shows the temperatures at different locations along the diametrical axis for all the cases mentioned in table 3.1 for both EDM process and cryogenic assisted EDM process. The position r = 0 (centre of the electrode) depicts the location where maximum heat flux is applied and r = R (where R is the radius of the electrode) depicts the location at the edge of the electrode as shown in figure 3.3. Again it is clearly evident that the temperature is lesser in cryogenic assisted EDM process as compared to EDM process due to cryogenic cooling. The temperature distribution plots for each case are shown in table 3.6.

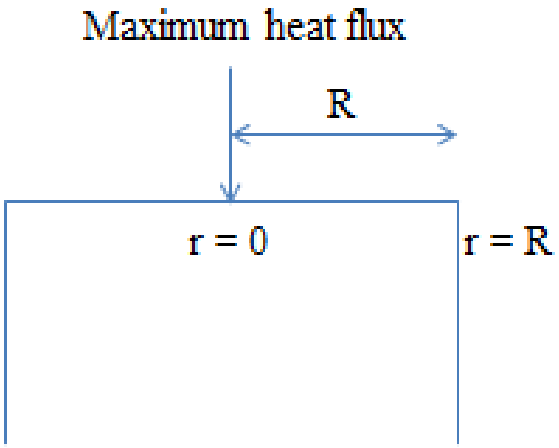

Figure 3.3: Location of the points in the analysis of temperature along diametrical axis

Table 3.6: Temperature distribution plots along diametrical axis for conventional EDM process and cryogenic assisted EDM process.

S.No.	CONVENTIONAL EDM PROCESS	CRYOGENIC ASSISTED EDM PROCESS
1	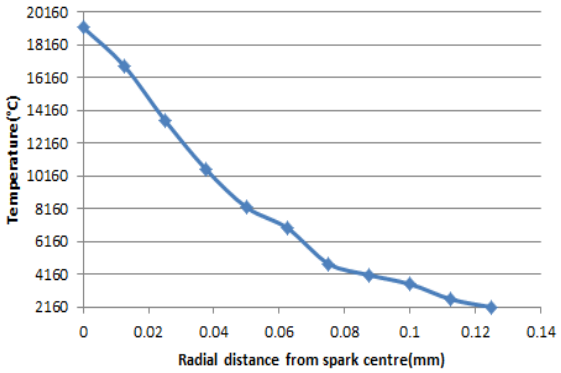	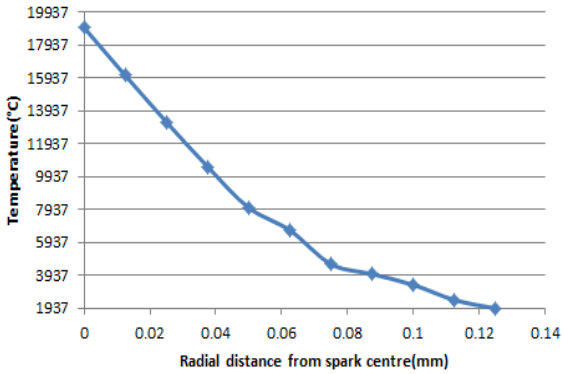

S.No.	CONVENTIONAL EDM PROCESS	CRYOGENIC ASSISTED EDM PROCESS
2	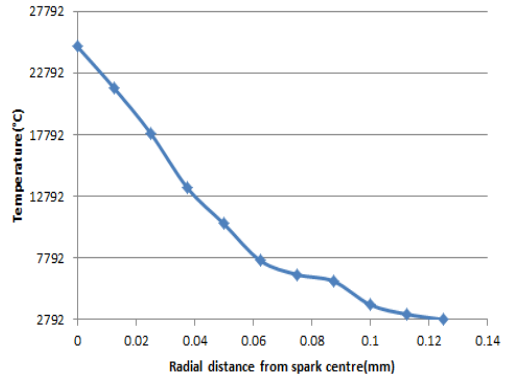	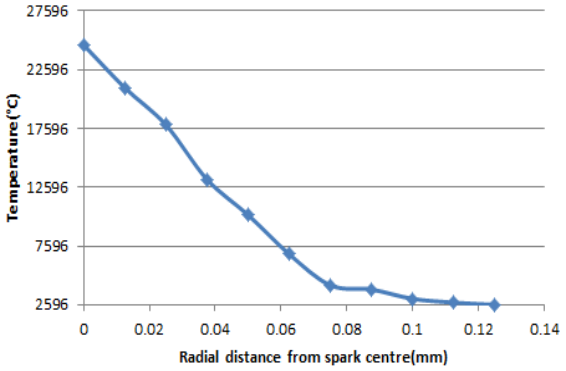
3	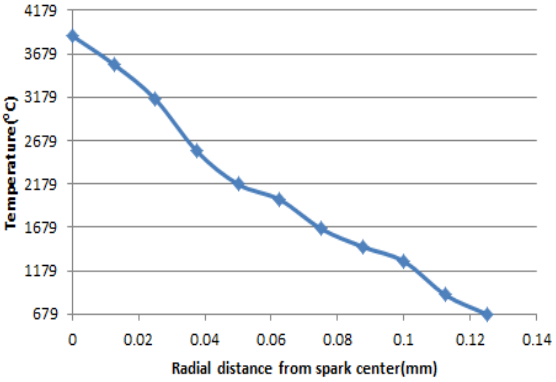	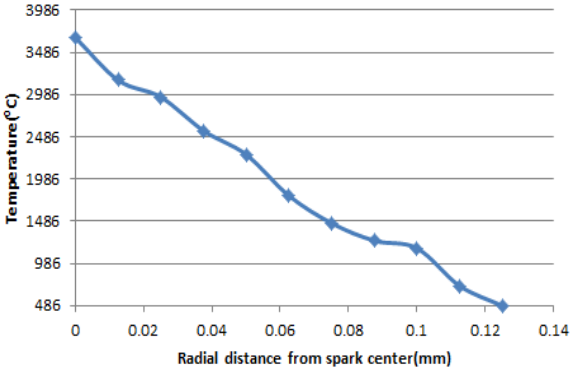
4	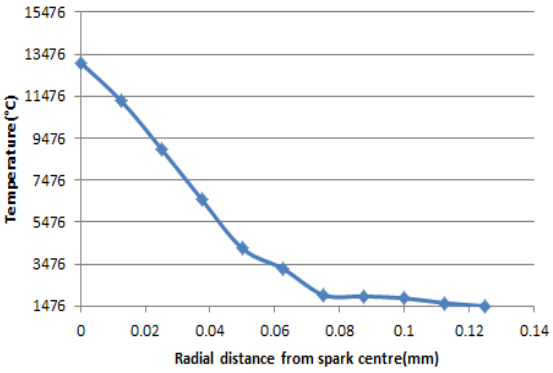	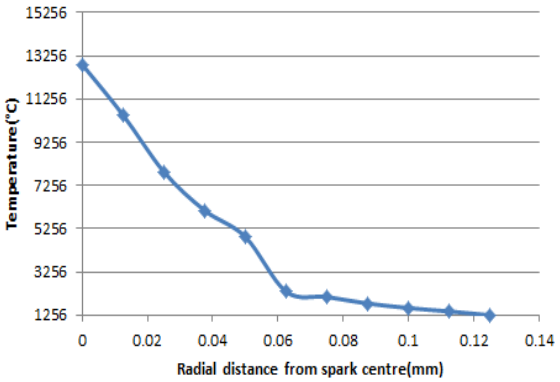
5	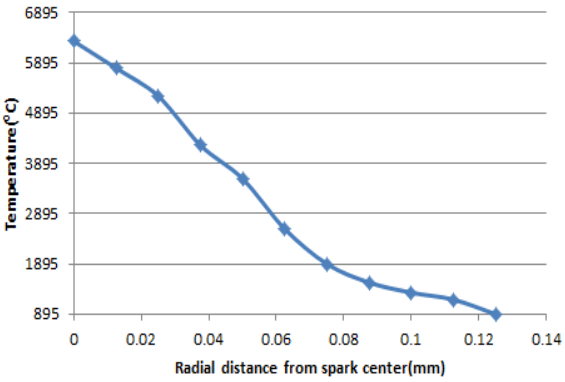	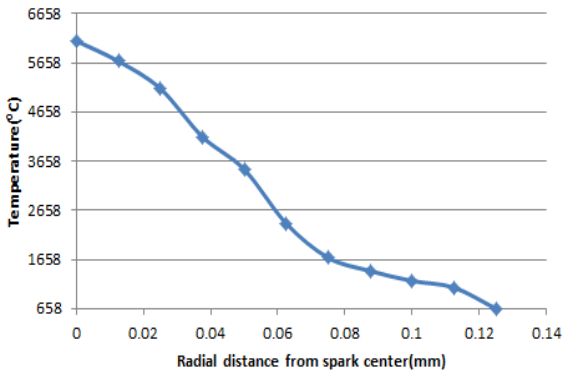

S.No.	CONVENTIONAL EDM PROCESS	CRYOGENIC ASSISTED EDM PROCESS
6	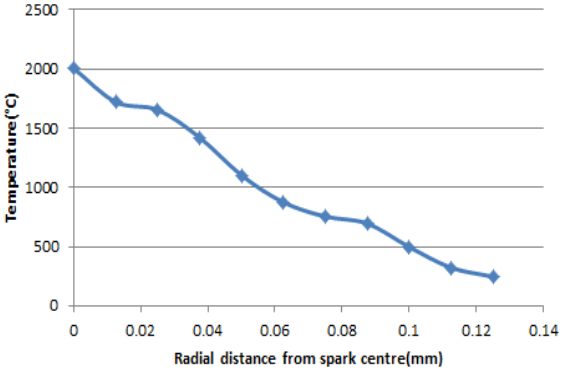	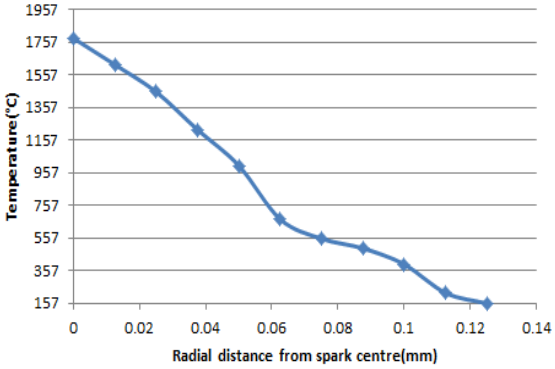
7	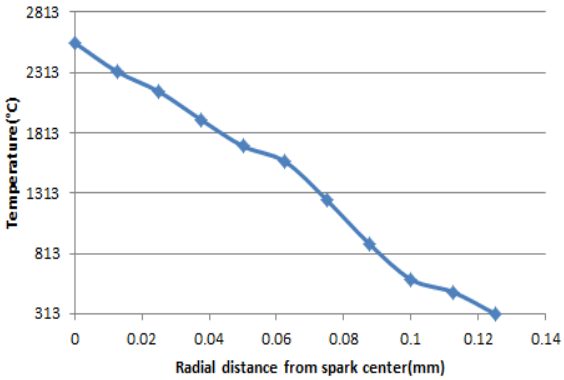	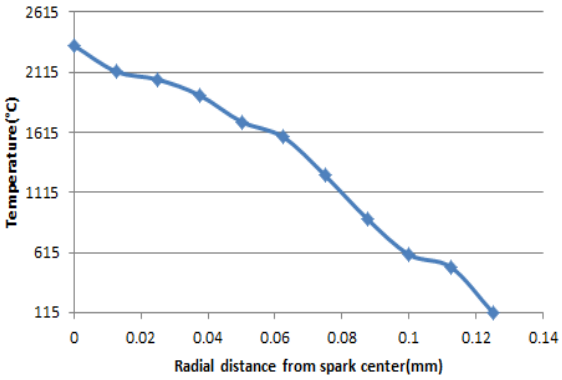
8	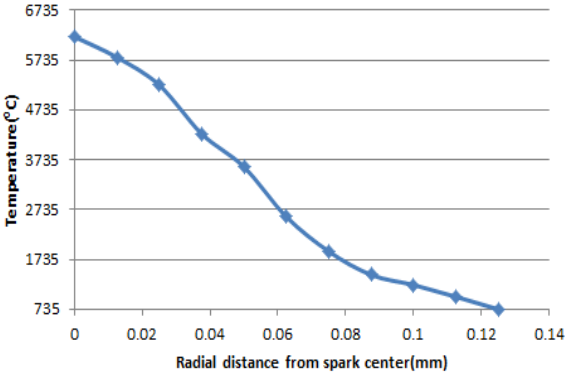	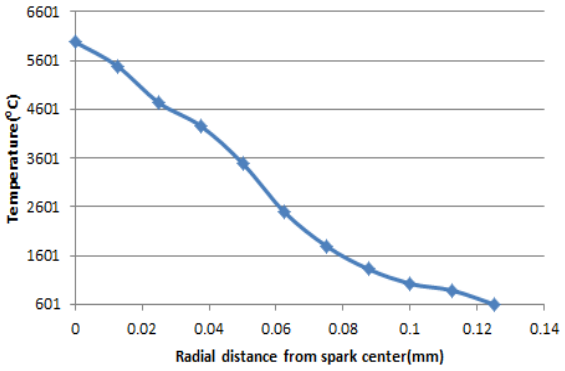
9	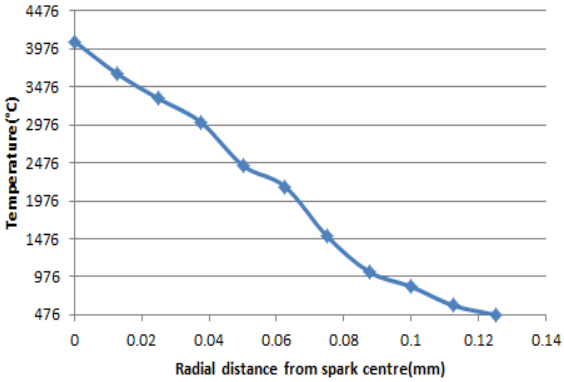	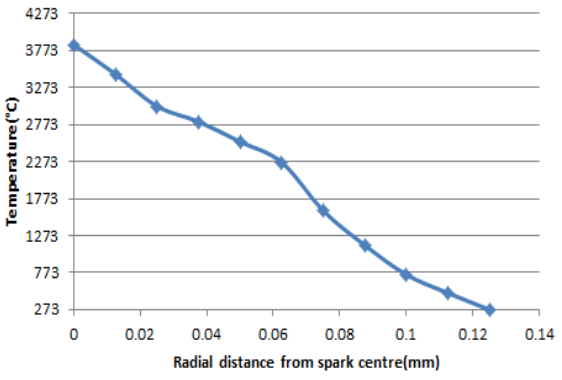

S.No.	CONVENTIONAL EDM PROCESS	CRYOGENIC ASSISTED EDM PROCESS
10	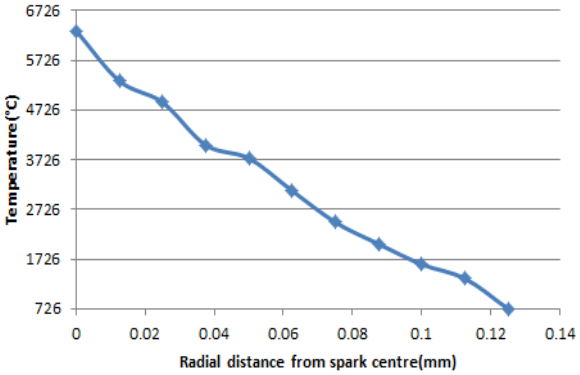	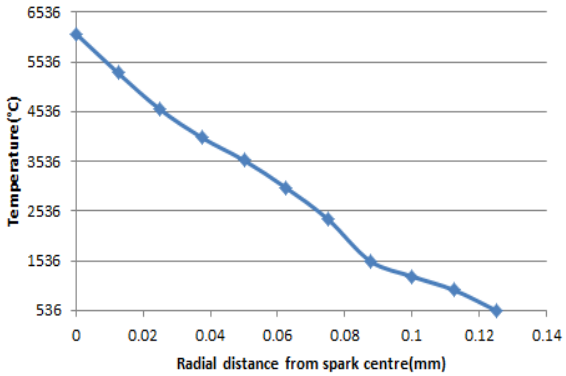
11	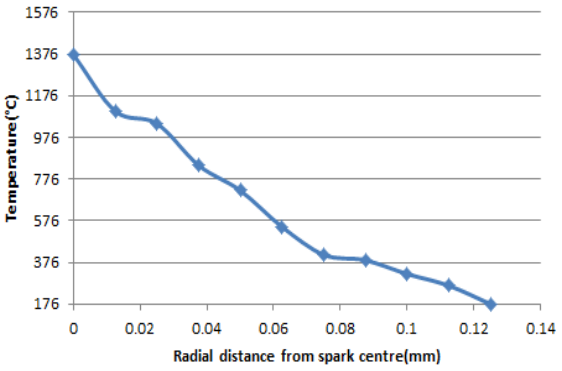	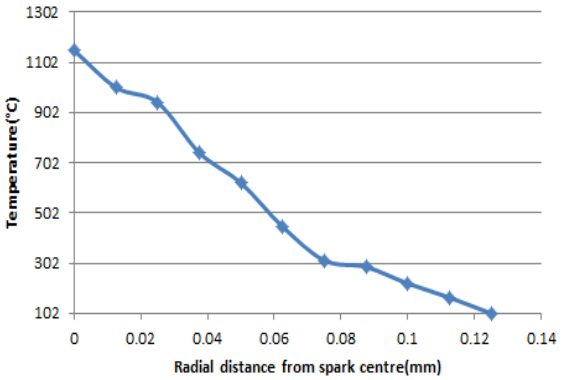
12	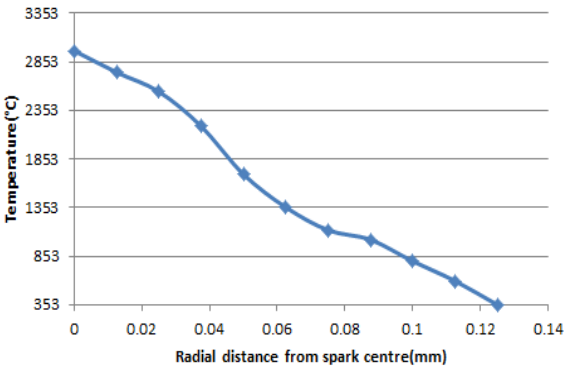	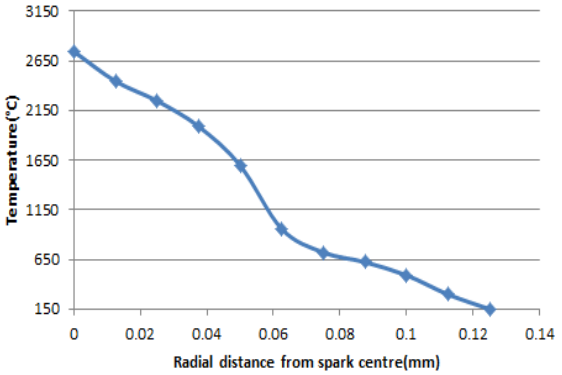
13	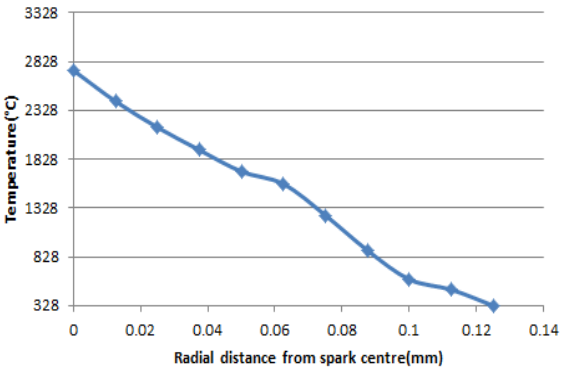	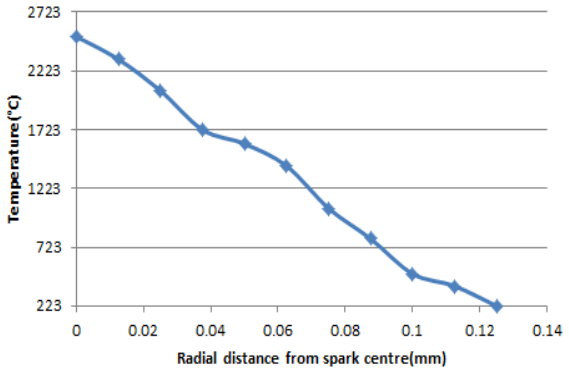

S.No.	CONVENTIONAL EDM PROCESS	CRYOGENIC ASSISTED EDM PROCESS
14	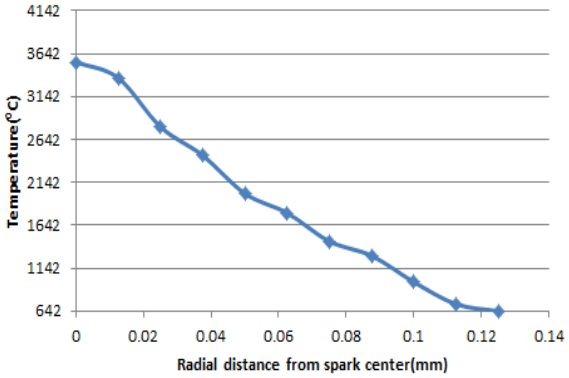	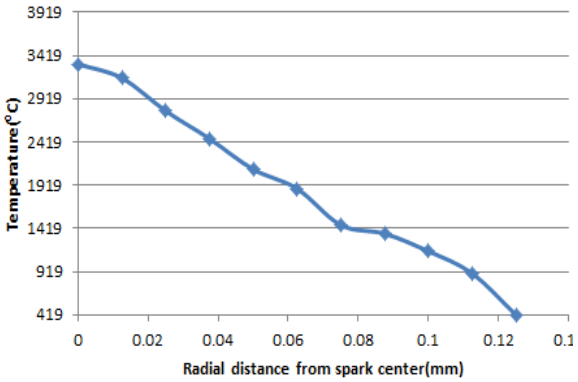
15	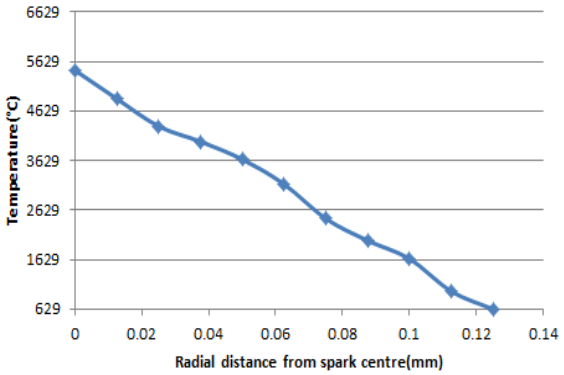	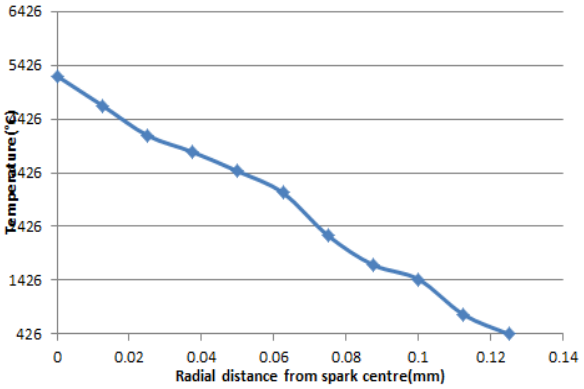

CHAPTER 4

THERMAL ANALYSIS OF CRYOGENIC ASSISTED EDM PROCESS AND EDM PROCESS

During the EDM process, discharge phenomenon occurs for a very short period of time in a narrow space filled with dielectric fluid. Occurrence of spark causes evaporation and melting of the material from the electrode. Due to the complex nature of the process, it is difficult to observe the process experimentally and quantify the mechanism of material removal. Mathematical models are required for accurate prediction of crater shapes and tool wear rate (TWR). For the thermal analysis of the process, conduction is considered as the primary mode of heat transfer between the plasma and the workpiece or tool.

4.1 ASSUMPTIONS

A 2D axi-symmetric thermal finite element model of single-spark EDM process has been developed based on assumptions such as Gaussian distribution of heat flux, time dependent spark radius, etc. to predict the shape of crater cavity, material removal rate and tool wear rate. The following assumptions have been made for the thermal modeling.

- Tool material is homogeneous and isotropic in nature.
- The material properties of the tool are temperature dependent.
- Heat transfer is purely by conduction.
- EDM spark channel is considered as a cylindrical column.
- The spark radius is a function of discharge duration.
- The model is developed for a single spark.
- Only a fraction of total spark energy is dissipated as heat into the tool.
- Heat flux is assumed to be Gaussian-distributed.
- The fraction of the energy that is transferred into the tool is constant during the pulse.
- The current intensity and discharge voltage are assumed constant during the pulse.

4.2 GOVERNING EQUATION

Fourier heat conduction equation is taken as the governing equation and is given below [31].

$$\frac{\partial^2 T}{\partial r^2} + \frac{1}{r}\left(\frac{\partial T}{\partial r}\right) + \frac{\partial^2 T}{\partial z^2} = \frac{\rho C_p}{K}\left(\frac{\partial T}{\partial t}\right) \ldots\ldots\ldots\ldots\ldots\ldots\ldots\ldots\ldots\ldots\ldots (4.1)$$

Where r and z are the cylindrical coordinates of work space; T is temperature; K is thermal conductivity; ρ is density; Cp is specific heat capacity of material and t is time.

4.3 RADIUS OF SPARK

The spark radius which indicates the size of heat flux on the tool surface is an important factor in the modeling of the EDM process. It is extremely difficult to experimentally measure spark radius due to very short pulse duration of the order of microseconds. Eubank et al. [25] considered variable mass cylindrical plasma model which shows the dependence of plasma radius on discharge duration. In the present work, the equation used to calculate spark radius at cathode and anode is given below.

$$R_p = 0.788 \times (T_{on})^{0.75} \ldots\ldots\ldots\ldots\ldots\ldots\ldots\ldots\ldots\ldots\ldots\ldots (4.2)$$

Where Ton indicates the spark on time and Rp is spark radius. Figure 4.1 shows the variation of spark radius with pulse on time.

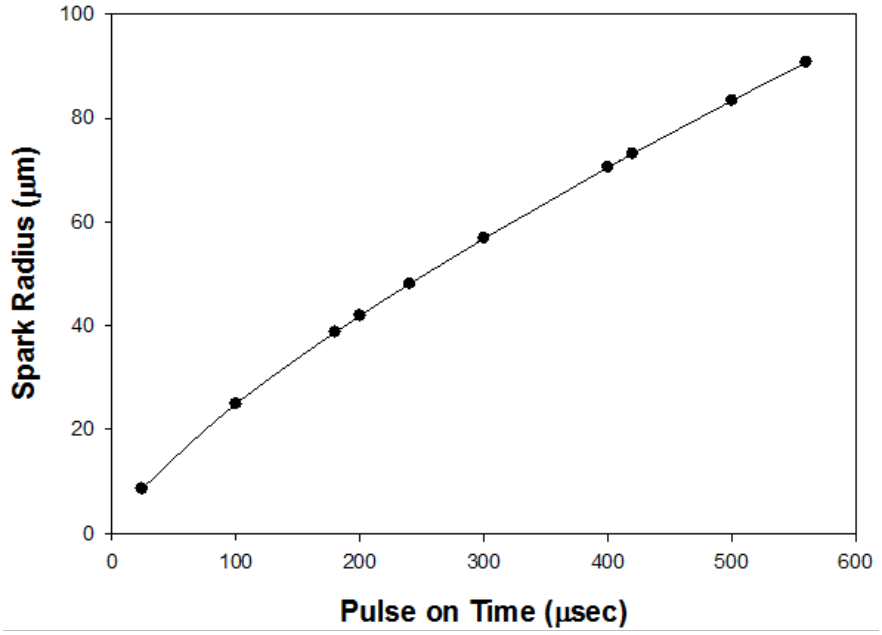

Figure 4.1: Variation of spark radius with pulse on time

4.4 ENERGY DISTRIBUTION IN EDM

Distribution of spark energy is other important consideration in the thermal analysis of EDM process. The total energy gets divided into three parts, a part of

energy is conducted away by the cathode, other part is conducted away by the anode, and the rest is dissipated in the dielectric. Dibitonto et al. [23] used experimental data that was gathered for different discharge duration and current values which indicate that the fraction of the total heat that goes into the cathode (Fc) is about 18%, the amount of heat absorbed by the anode (Fa) is about 8 %, the rest of the heat dissipated into the dielectric medium. In the present work, the same values of Fc and Fa have been considered.

4.5 HEAT OF A SPARK

It is imperative to model the heat input which is generated by single discharge before generating the numerical solution of the equation of the thermal problem. The heat input is defined by its shape and the amount of heat that is applied to the workpiece. In this present work, the Gaussian heat input model has been used to approximate the heat from the plasma. As Dibitonto et al. [23] mentioned, although the point heat source approximation or uniformly distributed heat flux model is acceptable for analytical work, the Gaussian model still remains the best approximation of the heat input. The Gaussian model has two factors, the fraction of heat applied to the workpiece and the radius of the area heated by the plasma. The prediction of material removal rate in single spark EDM model depend on the amount of heat input, radius of spark and thermo-physical properties of material. The heat flux q(r) entering the workpiece due to EDM spark [23] is represented by equation 4.2.

$$q(r) = q_0 e^{\left\{-4.5\left(\frac{r}{R_p}\right)^2\right\}} \quad \ldots\ldots\ldots\ldots\ldots\ldots\ldots\ldots\ldots\ldots\ldots\ldots\ldots\ldots (4.3)$$

Where ‘r’ is the radial distance at any point from the centre of the spark and Rp is the spark radius or plasma radius. The maximum heat flux qo can be calculated by equation 4.3.

$$q_0 = \frac{4.56 \times F_c \times V \times I}{\pi R_p^2} \quad \ldots\ldots\ldots\ldots\ldots\ldots\ldots\ldots\ldots\ldots\ldots\ldots\ldots\ldots (4.4)$$

Where Fc is the fraction of total energy going to the cathode, V is discharge voltage (V), I is current (A) and Rp (μm) is spark radius at the work surface. In present analysis discharge voltage is taken as 25V. Figure 4.2 shows variation of the heats flux as the plasma channel expands with time, as the plasma channel becomes wider the heat flux distribution becomes less steep. Figure 4.3 shows the variation of heat flux with respect to spark radius.

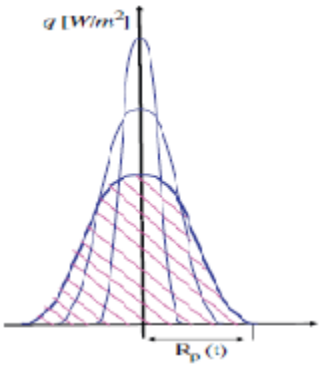

Figure 4.2: Variation of heat flux with spark radius [33].

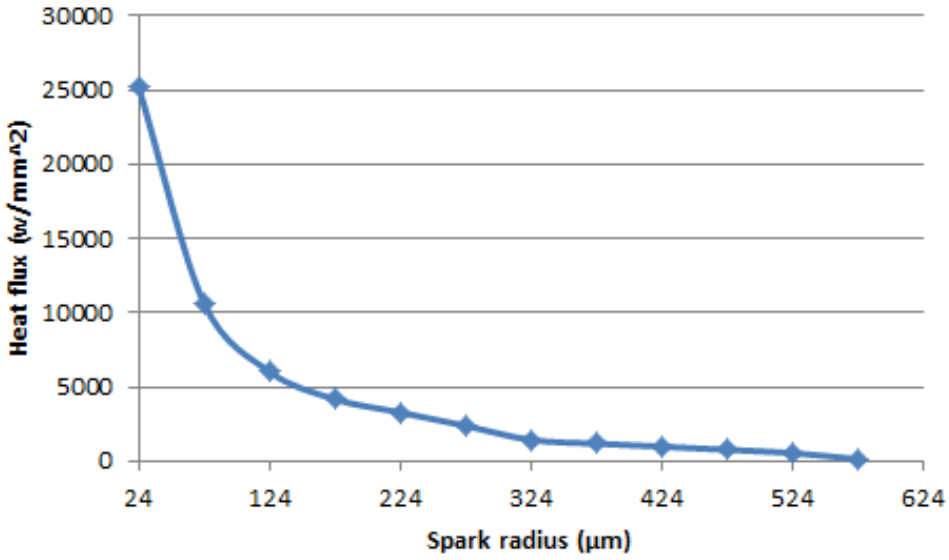

Figure 4.3: Variation of heat flux with respect to spark radius

4.6 BOUNDARY CONDITIONS

In EDM process, the tool is immersed in dielectric medium; the temperature of the domain is thus assumed to be ambient temperature (To) initially. The boundaries of the domain away from the spark are considered as insulated. A small cylindrical portion of the workpiece around the spark is used as the domain.

Initial condition is,

when, t = 0, $T=To$

Boundary conditions are

when, $0 < t \leq$ Ton

$$-K\left(\frac{\partial T}{\partial z}\right) = q(r)\ for\ 0 < r < R_p$$

$$-K\left(\frac{\partial T}{\partial z}\right) = 0\ for\ r > R_p$$

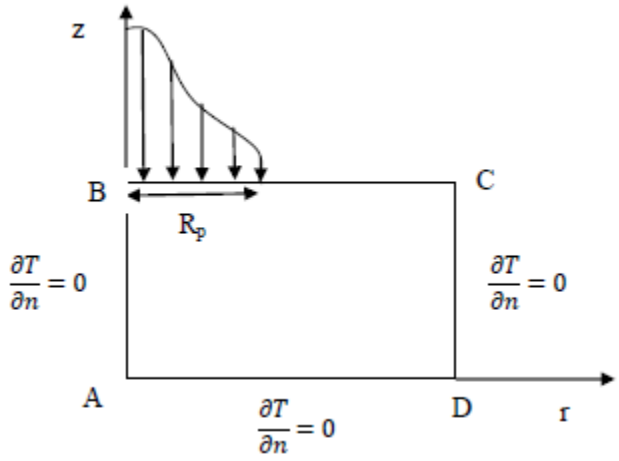

Figure 4.4: Boundary conditions for thermal analysis

Heat flux (q) is applied on the top surface BC of the workpiece where the spark occurs. Further, the boundaries AD and CD are at such distances that it is assumed that there is no heat transfer across them. The boundary AB is an axis of symmetry. Figure 4.4 shows the associated boundary conditions applied on thermal model.

4.7 METHODOLOGY OF ANALYSIS OF THERMAL MODEL

The governing equation with boundary conditions as mentioned above is solved by finite element method to predict the temperature distribution with the heat flux at the spark location and the discharge duration as the total time step. The analysis of the model was carried out using ANSYS software. A three-dimensional model was created for thermal analysis. The domain is discritized by unstructured mesh with TET element. Considering the variation of thermo-physical properties over a temperature range from ambient to melting point, effective values are used for density, thermal conductivity and specific heat. The effective values used were values averaged over the entire temperature range rather than a single value at average temperature as used by Dibitonto et al. [23]. Table 4.1 shows the material properties used in present analysis. Convergence condition was tested by increasing the number of elements in the mesh and a converged mesh of 38398 elements has been considered in this study. Figure 4.5 shows the three-dimensional expanded meshed model and the refined mesh. Refinement of meshing has been done in the area where heat flux is to be applied. Figure 4.6 shows the temperature distribution profile and crater shape for typical operating condition. Figure 4.7 shows the temperature distribution on tool after the discharge duration for different operating conditions for both EDM process and cryogenic assisted EDM process.

Table 4.1: Material properties used for thermal analysis

S. No.	Material	Density (kg/m^3)	Thermal conductivity (W/m)	Specific heat (J/kg-K)	Melting point (°C)
1	Copper	8640	367	438	1083

a) b)

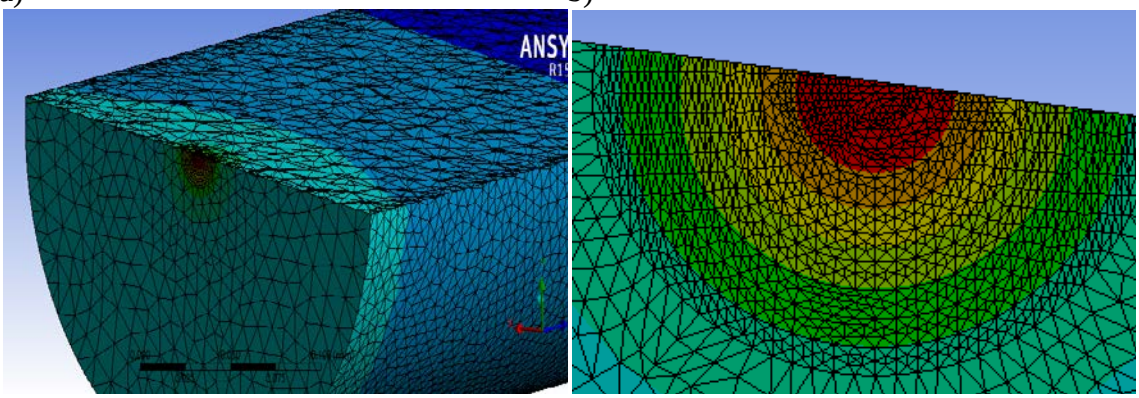

Figure 4.5: a) Three-dimensional expanded meshed model b) The refined mesh

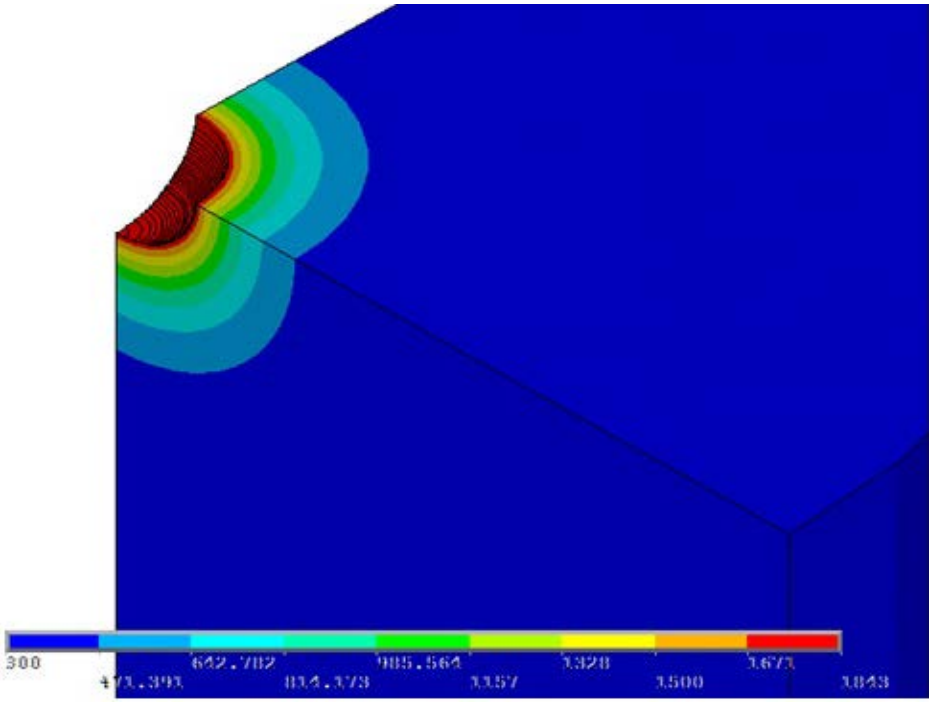

Figure 4.6: Temperature distribution profile and crater shape for typical operating condition

CASE	CONVENTIONAL EDM PROCESS	CRYOGENIC ASSISTED EDM PROCESS
I = 4A, Ton = 200µs	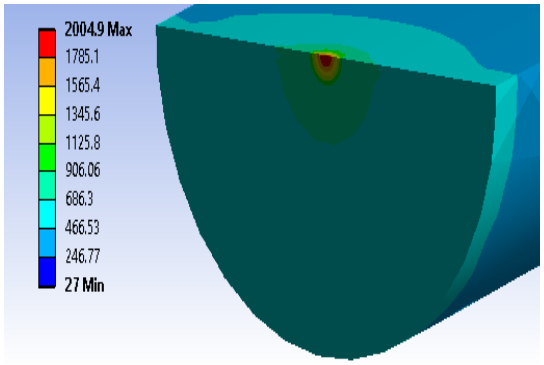	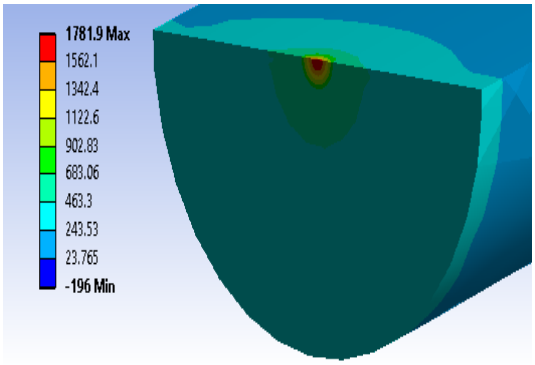
I = 5A, Ton = 300µs	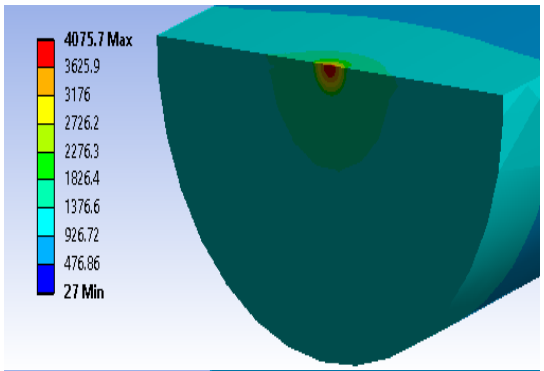	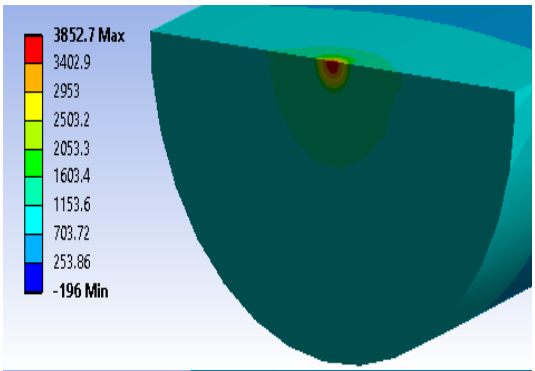
I = 6A, Ton = 400µs	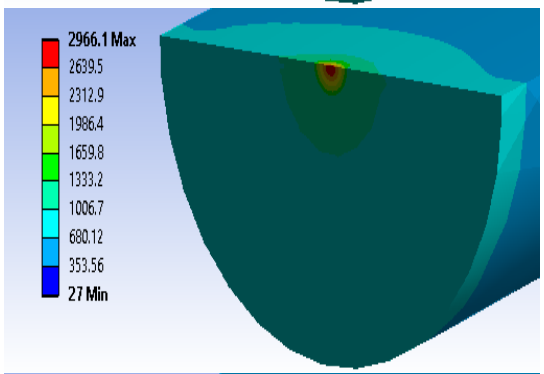	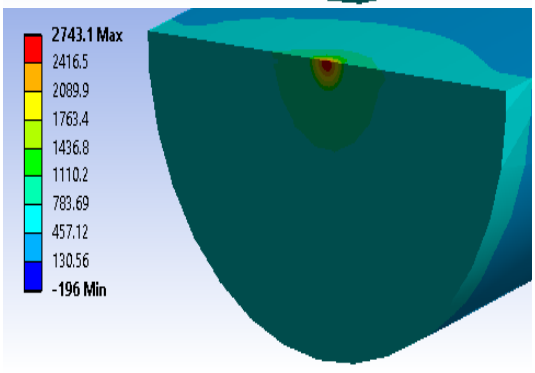
I = 7A, Ton = 300µs	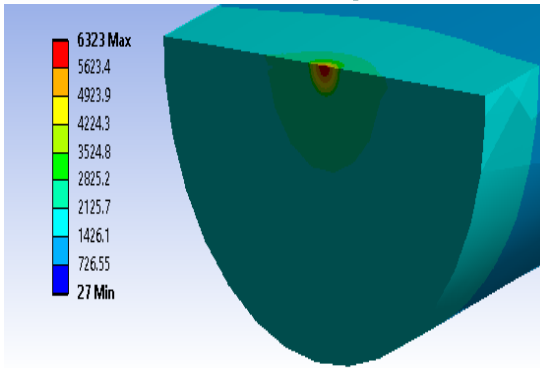	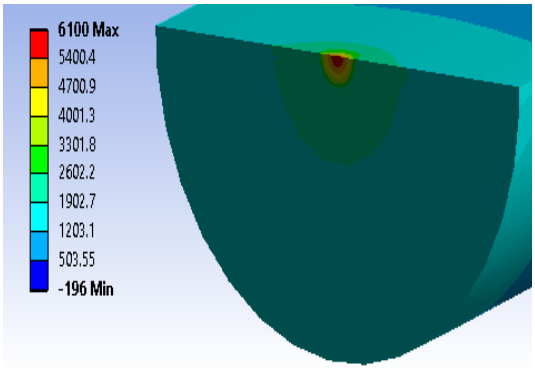

Figure 4.7: Temperature distribution on tool for different operating conditions

4.7.1 CALCULATION OF RADIUS AND DEPTH OF CRATER

The temperature distribution along the diameter of the tool electrode at the surface of the electrode has also been obtained for both EDM process and cryogenic assisted EDM process. Here, the known input heat flux was discretised in 10 parts on the

geometry of circular cross-section. The spark radius obtained by the equation 4.2 was also divided into 10 equal sections. Now the flux distribution in each segment was calculated by equation 4.3 and applied accordingly as shown in figure 4.8.

Figure 4.8: Different Heat Fluxes applied on different locations following Gaussian distribution

The simulations were performed according to the pre-decided boundary conditions. The details of each node, containing information of the nodal coordinates and the temperature derived from the simulation, was transferred to an excel file. This file (called as F1) was sorted for the temperature. Further all the elements which had temperature either equal to or greater than the melting point of the electrode were selected and transferred to another file (called as F2). Now all the temperature along x-axis which have y and z coordinates as zero (0) were selected and transferred to another file (called as F3). Then an algorithm was created which read the sorted file as the input and generated a distribution across the x axis shown in figure 4.9. This distribution was sorted based on average value at the location to obtain a new graph which highlighted the stabilization of the temperature from maximum temperature to the melting temperature. This graph is given in figure 4.10. This also highlights the maximum distance of the crater from the centre of the applied flux induced. This maximum distance is called as the radius of crater. Table 4.2 shows the radius of crater values for different cases for both EDM process and cryogenic assisted EDM process.

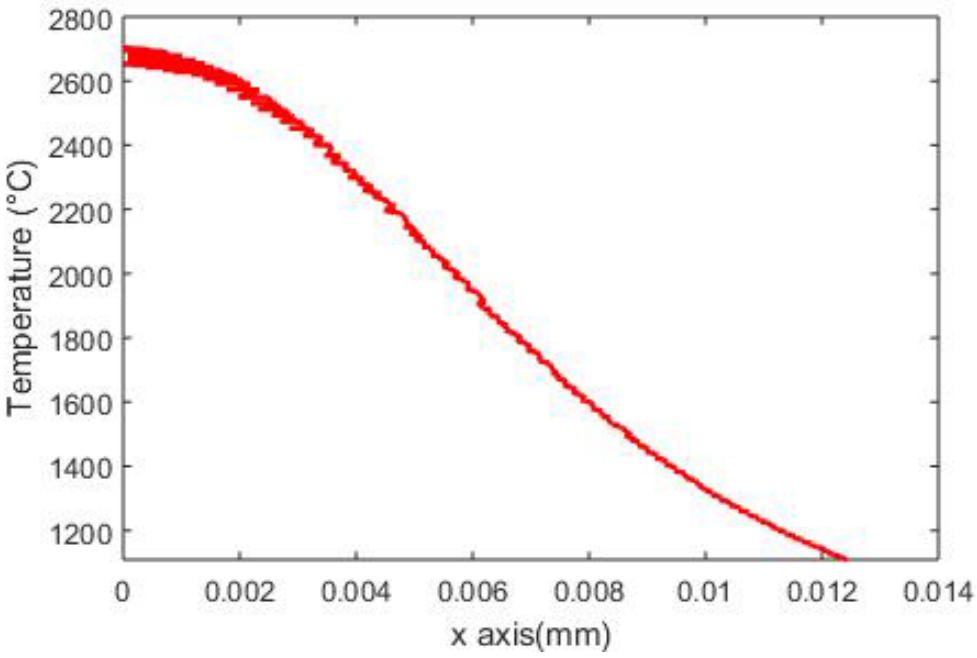

Figure 4.9: Temperature distribution across x axis generated by algorithm

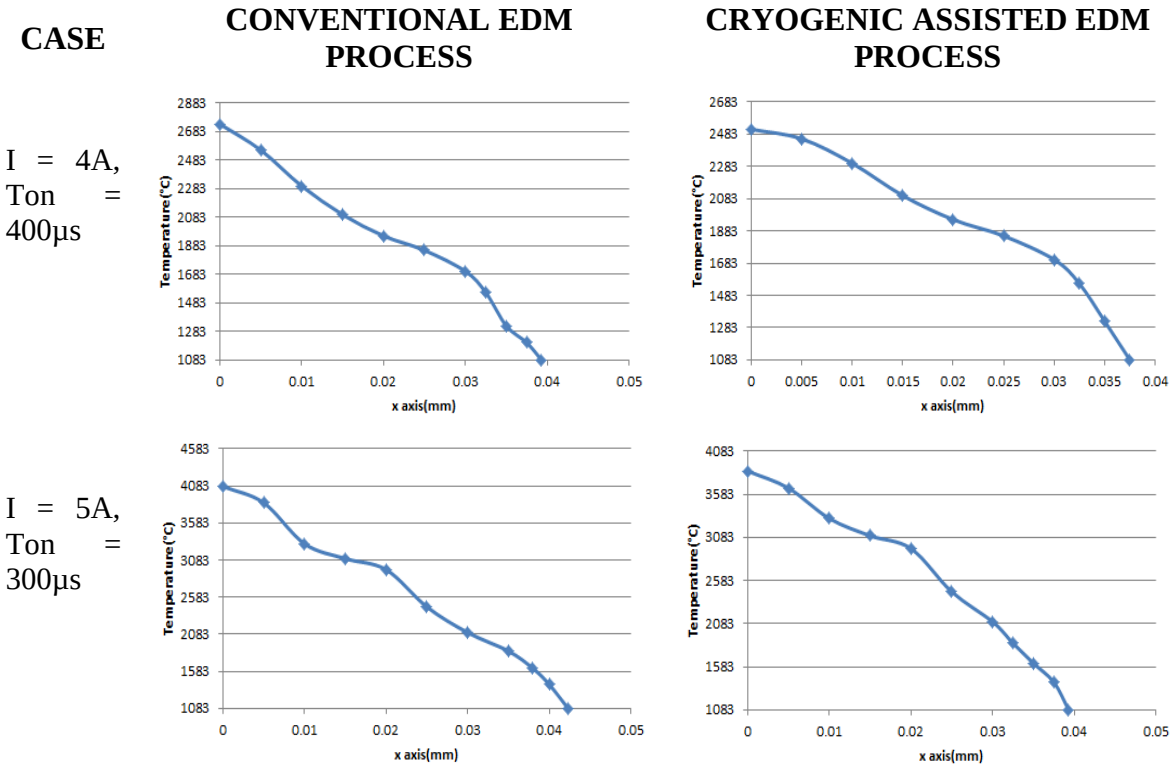

Figure 4.10: Temperature distribution from maximum temperature to melting temperature along x axis

Table 4.2: Values of radius of crater for conventional EDM process and cryogenic assisted EDM process in different cases

S.No.	PULSE ON TIME (µS)	PULSE OFF TIME (µS)	DISCHARGE CURRENT (A)	RADIUS OF CRATER (in mm)	
				CONVENTIONAL EDM PROCESS	CRYOGENIC ASSISTED EDM PROCESS
1	24	2.4	8.5	0.02755	0.02389
2	100	44	5	0.04289	0.02580
3	180	4.2	36	0.03298	0.02913
4	200	120	4	0.02932	0.02332
5	240	5.6	44	0.03158	0.02722
6	300	132	5	0.04232	0.03911
7	300	132	7	0.04712	0.04205
8	400	112	6	0.03754	0.03501
9	400	112	4	0.03932	0.03750
10	420	7.5	58	0.05315	0.04755
11	500	220	5	0.04298	0.03313
12	560	10	68	0.01246	0.01020

Similarly in file F2, now all the temperature along z-axis which have x and y coordinates as zero (0) were selected and transferred to another file (called as F4). Then an algorithm was created which read the sorted file as the input and generated a distribution across the z axis. This distribution was sorted based on average value at the location which highlighted the stabilization of the temperature from maximum temperature to the melting temperature. This graph is given in figure 4.11. This also highlights the maximum distance of the crater along the depth from the centre of the applied flux. This maximum distance is called as the depth of crater. Table 4.3 shows the depth of crater values for different cases for both EDM process and cryogenic assisted EDM process. Figure 4.12 and figure 4.13 shows the comparison of radius of crater and depth of crater between EDM and cryogenic assisted EDM processes. It can be observed that radius of crater and depth of crater is smaller in cryogenic

assisted EDM process. The flow chart of the developed algorithm has been provided in figure 4.14.

Table 4.3: Values of depth of crater for conventional EDM process and cryogenic assisted EDM process in different cases

S.No.	PULSE ON TIME (µS)	PULSE OFF TIME (µS)	DISCHARGE CURRENT (A)	DEPTH OF CRATER (in mm)	
				CONVENTIONAL EDM PROCESS	CRYOGENIC ASSISTED EDM PROCESS
1	24	2.4	8.5	0.02411	0.02140
2	100	44	5	0.01819	0.01623
3	180	4.2	36	0.02843	0.02364
4	200	120	4	0.02520	0.02129
5	240	5.6	44	0.02258	0.01933
6	300	132	5	0.03045	0.02745
7	300	132	7	0.03195	0.02856
8	400	112	6	0.02580	0.02280
9	400	112	4	0.03332	0.03102
10	420	7.5	58	0.02895	0.02468
11	500	220	5	0.02943	0.02454
12	560	10	68	0.00980	0.00650

CASE

I = 4A, Ton = 400µs

CONVENTIONAL EDM PROCESS

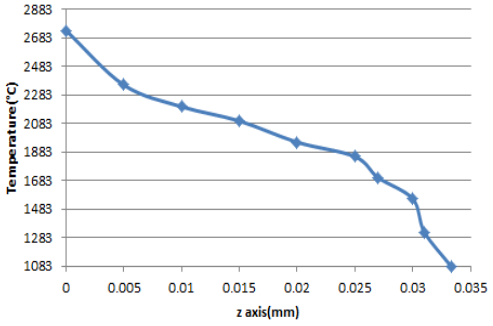

CRYOGENIC ASSISTED EDM PROCESS

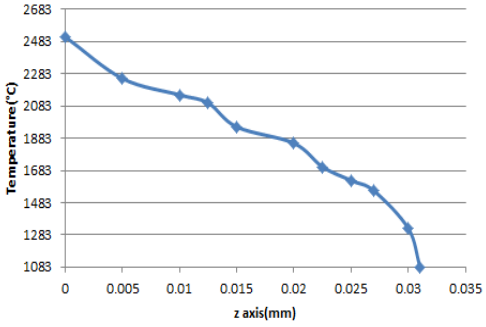

I = 5A, Ton = 300µs

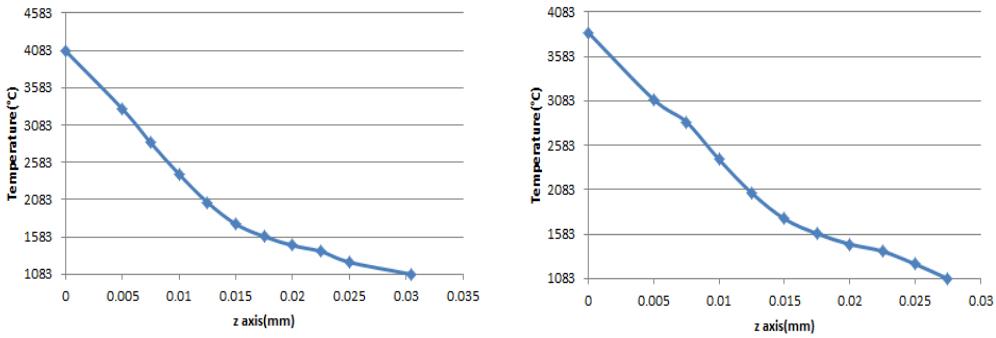

Figure 4.11: Temperature distribution from maximum temperature to melting temperature along z axis

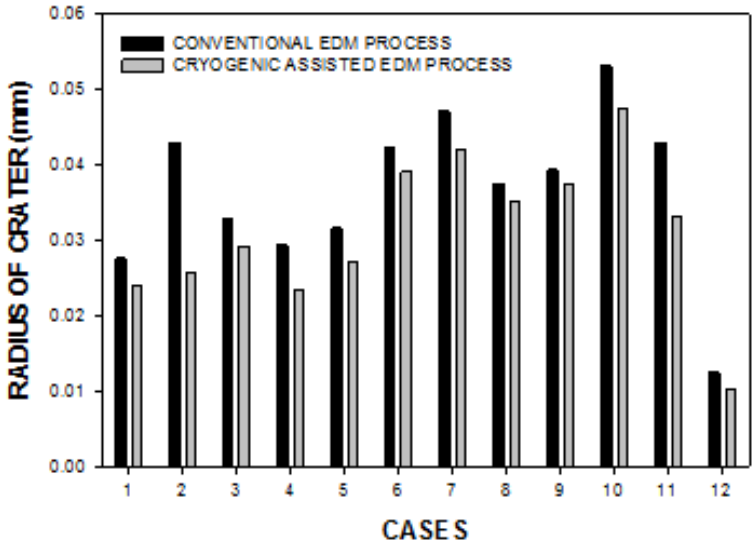

Figure 4.12: Comparison of radius of crater between conventional EDM and cryogenic assisted EDM processes

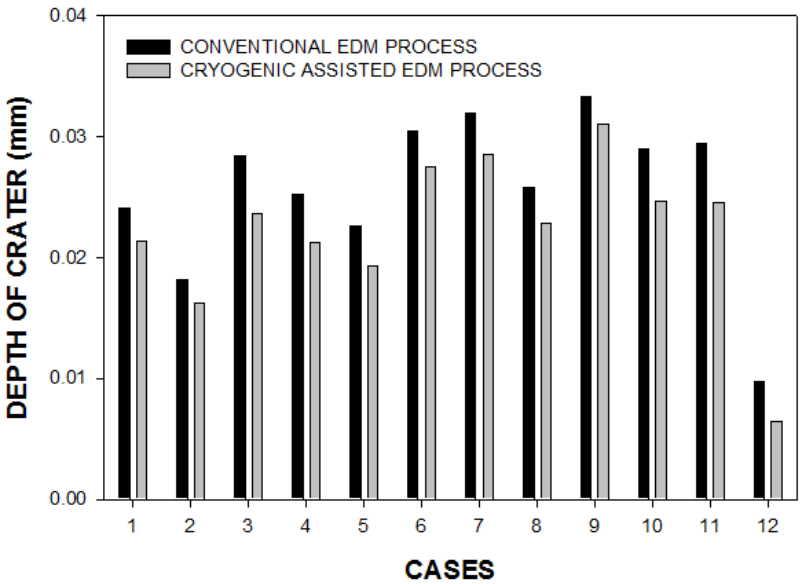

Figure 4.13: Comparison of depth of crater between conventional EDM and cryogenic assisted EDM processes

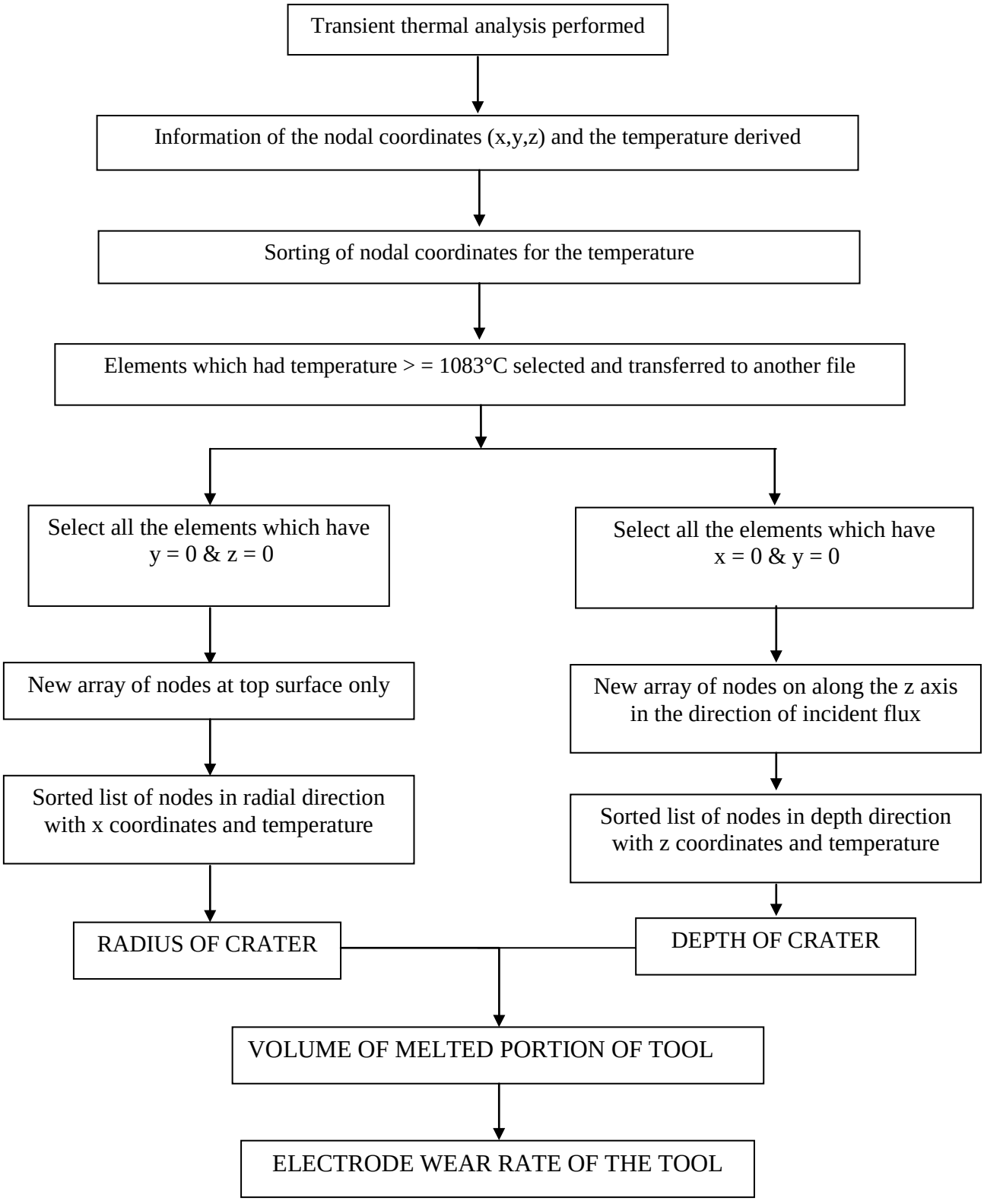

Figure 4.14: Algorithm for extraction of nodal coordinates and temperatures above melting temperature to evaluate electrode wear of the tool

4.7.2 CALCULATION OF VOLUME OF MELTED PORTION OF TOOL ELECTRODE

Volume of melted portion of tool electrode is given by,

$$V_t = \frac{\pi h}{6}(3r^2 + h^2) \dots\dots\dots\dots\dots\dots\dots\dots\dots\dots\dots\dots\dots\dots\dots.. (4.5)$$

Where ‘r’ is radius of melted tool and ‘h’ is depth of melted tool electrode.

The value of radius and depth of melted portion of tool electrode for both EDM process and cryogenic assisted EDM process have been obtained through thermal analysis and are provided in table 4.2 and 4.3. Table 4.4 shows the maximum temperature and tool wear rate for various operating conditions. Figure 4.15 shows the comparison of volume of melted portion of tool electrode between EDM and cryogenic assisted EDM processes. It can be observed that volume of melted portion of tool electrode is smaller in cryogenic assisted EDM process.

Table 4.4: Values of volume of melted portion of tool electrode for conventional EDM process and cryogenic assisted EDM process in different cases

S.No.	PULSE ON TIME (μS)	PULSE OFF TIME (μS)	DISCHARGE CURRENT (A)	VOLUME OF MELTED PORTION (in mm^3)	
				CONVENTIONAL EDM PROCESS	CRYOGENIC ASSISTED EDM PROCESS
1	24	2.4	8.5	0.0000361	0.0000243
2	100	44	5	0.0000557	0.0000192
3	180	4.2	36	0.0000606	0.0000384
4	200	120	4	0.0000424	0.0000232
5	240	5.6	44	0.0000414	0.0000263
6	300	132	5	0.0001000	0.0000767
7	300	132	7	0.0001280	0.0000915
8	400	112	6	0.0000661	0.0000501
9	400	112	4	0.0001000	0.0000841
10	420	7.5	58	0.0001410	0.0000955
11	500	220	5	0.0000987	0.0000500
12	560	10	68	0.0000288	0.0000121

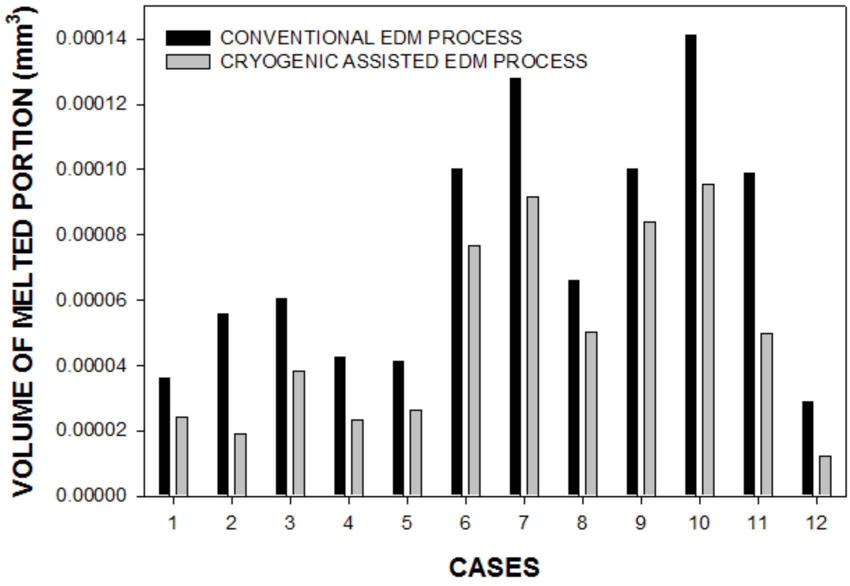

Figure 4.15: Comparison of that volume of melted portion of tool electrode between conventional EDM and cryogenic assisted EDM processes

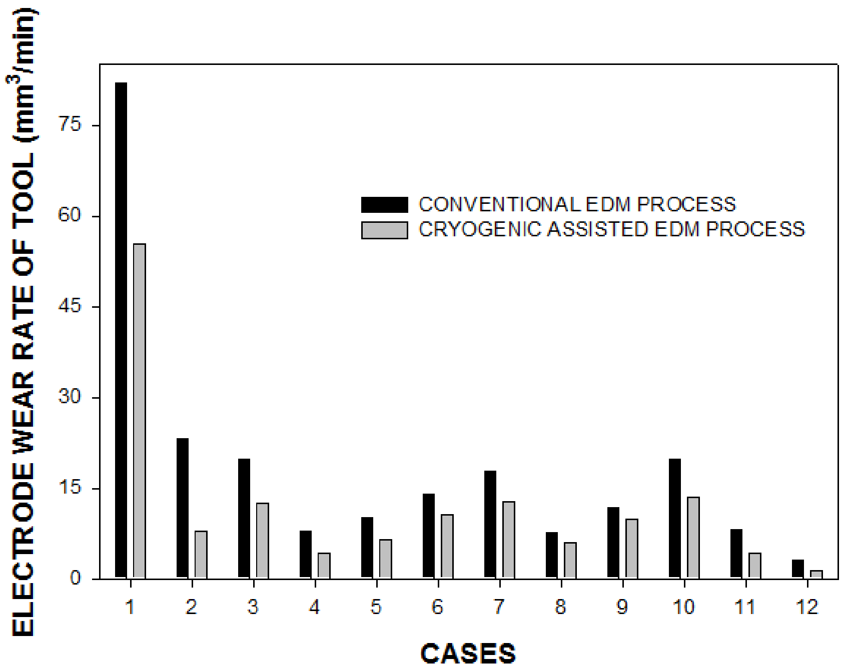

Figure 4.16: Comparison of electrode wear rate of tool between conventional EDM and cryogenic assisted EDM processes

4.7.3 CALCULATION OF ELECTRODE WEAR RATE OF THE TOOL

The electrode wear rate of the tool is given by,

$$EWR = \frac{V_t}{(T_{on} + T_{off})} \dots\dots\dots\dots\dots\dots\dots\dots\dots\dots\dots\dots\dots\dots\dots\dots (4.6)$$

Where 'V_t' is the volume of melted tool, T_{on} is the duration of discharge and Toff is the period when the spark is off.

The value of t_{on} and t_{off} have been considered from the various test conditions and volume of melted portion of tool electrode for both EDM process and cryogenic assisted EDM process are provided in table 4.4. Table 4.5 shows the electrode wear rate of the tool for various operating conditions for both EDM process and cryogenic assisted EDM process. Figure 4.16 shows the comparison of of electrode wear rate of the tool between EDM and cryogenic assisted EDM processes. It can be observed that of electrode wear rate of the tool is smaller in cryogenic assisted EDM process.

Table 4.5: Values of electrode wear rate of tool for conventional EDM process and cryogenic assisted EDM process in different cases

S.No.	PULSE ON TIME (µS)	PULSE OFF TIME (µS)	DISCHARGE CURRENT (A)	ELECTRODE WEAR RATE OF TOOL (in mm^3/min)	
				CONVENTIONAL EDM PROCESS	CRYOGENIC ASSISTED EDM PROCESS
1	24	2.4	8.5	81.96	55.23
2	100	44	5	23.21	7.99
3	180	4.2	36	19.73	12.51
4	200	120	4	7.94	4.35
5	240	5.6	44	10.12	6.41
6	300	132	5	13.94	10.65
7	300	132	7	17.83	12.71
8	400	112	6	7.74	5.86
9	400	112	4	11.74	9.85
10	420	7.5	58	19.80	13.42
11	500	220	5	8.22	4.16
12	560	10	68	3.03	1.27

Chapter 5

SUMMARY, CONCLUSIONS AND SCOPE FOR FUTURE WORK

5.1 SUMMARY

Being a thermal process, EDM is unavoidably accompanied with high rates of electrode wear which requires more number of electrodes to be fabricated for a job. In EDM, the cost of machining also increases as the manufacturing of electrodes accounts for over 70% of the total machining cost [19]. The rapid electrode wear could be reduced by an efficient cooling strategy. An attempt of liquid nitrogen cooled electrode has shown to control electrode wear. The finite element based approach has been carried out to obtain the temperature profile at various points on the tool electrode. The analysis has been performed across the diameter and along the length of the electrode to gain better understanding of the temperature distribution. A comparative performance analysis of liquid nitrogen cooled electrode EDM and EDM has been attempted. For finite element analysis of EDM using liquid nitrogen cooled small diameter electrode, the temperature at the junction of liquid nitrogen with the electrode is taken as 77 K. The temperature of the electrode surface which is in contact with the dielectric is taken to be equal to room temperature that is 300 K. Further the spark radius and maximum heat flux supplied to tool electrode for different discharge current and discharge duration has been estimated. Convergence condition was tested by increasing the number of elements in the mesh. Based on this study, a converged mesh of 2228 elements has been considered. It has been clearly found that the temperature is lesser in cryogenic assisted EDM process as compared to EDM process, due to cryogenic cooling, both along the length of the electrode and along the diametrical axis of the electrode.

In the present work, an approach for the thermal modeling and simulation of EDM process and cryogenic assisted EDM process is developed using finite element method. Transient analysis of single spark has been done to predict the crater shape and volume of molten metal. The radius and depth of crater have been obtained with help of finite element approach. An algorithm has been developed to predict the radius and depth of crater. The radius and depth of crater indicates that the shape of molten metal is of hemisphere. Volume of molten metal in the tool electrode has been

obtained which further helps us to determine the electrode wear rate of the tool. This study was performed at different case studies for both EDM process and cryogenic assisted EDM process. It was found that the radius and depth of crater was lower in cryogenic assisted EDM process as compared to EDM process. This reduction varied from 5% to 40% for radius of crater and 7% to 34% in depth of crater. Further the volume of molten metal in tool electrode was lesser in cryogenic assisted EDM process. It was further observed that the electrode wear rate of cryogenic assisted EDM process was lesser as compared to EDM process. The variation in electrode wear rate of the tool was observed from 16% to 66%.

5.2 CONCLUSIONS

- Spark radius increases with increase in pulse on time.
- Heat flux reduces with increase in spark radius.
- The temperature is lesser in cryogenic assisted EDM process as compared to EDM process along the length of the electrode.
- The temperature is lesser in cryogenic assisted EDM process in comparison to EDM process along the diametrical axis of the electrode.
- Radius of crater was lower in cryogenic assisted EDM process. This reduction varied from 5% to 40% for radius of crater.
- Depth of crater was lower in cryogenic assisted EDM process as compared to EDM process and this reduction varied from 7% to 34%.
- The radius and depth of crater indicated that the shape of molten metal is of hemisphere.
- It was found that the volume of molten metal in tool electrode was lesser in cryogenic assisted EDM process.
- Electrode wear rate of cryogenic assisted EDM process was lesser as compared to EDM process by 16% to 66%.

5.3 SCOPE FOR FUTURE WORK

- Shape and size of the crater developed on the workpiece in cryogenic assisted EDM can be explored.
- The work can be extended to determine the temperature distribution and electrode wear rate in ultrasonic assisted cryogenically cooled EDM process.

REFERENCES

1. Y. Chen, S.M. Mahdavian, Analysis of electro-discharge machining process and its comparison with experiments, Journal of Materials Processing Technology 104 (2000) 150-157.
2. G. Boothroyd, W.A. Knight, Fundamentals of Machining and Machine Tools, Taylor & Francis, Florida, 2006.
3. K.H. Ho, S.T. Newman, State of the art electrical discharge machining (EDM), International Journal of Machine Tools and Manufacture, 43 (2003) 1287–1300.
4. N.M. Abbas, D.G. Solomon, M.F. Bahari, A review on current research trends in electrical discharge machining (EDM), International Journal of Machine Tools and Manufacture, 47 (2007) 1214–1228.
5. A.B. Puri, B. Bhattacharyya, An analysis and optimisation of the geometrical inaccuracy due to wire lag phenomenon in WEDM, International Journal of Machine Tools and Manufacture, 43(2) (2003) 151-159.
6. K.H. Ho, S.T. Newman, S. Rahimifard, R.D. Allen, State of the art wire electrical discharge machining (EDM), International Journal of Machine Tools and Manufacture, 44 (2004) 1247–1259.
7. P.K. Mishra, Nonconventional Machining, Narosa Publishing House, London, 1997.
8. K.M. Patel (2009). Experimental investigations into Electro Discharge Machining of TiC particles and SiC whiskers reinforced Alumina ceramic composite, PhD diss., Indian Institute of Technology Delhi, India
9. D. Kremer, J.L. Lebrun, B. Hosari, A. Moisan, Effects of Ultrasonic Viberations on the Performances in EDM. Annals of the CIRP, 38(1) (1989) 199-202.
10. M. Kunieda, S. Furuoya, N. Taniguchi, Improvement of EDM efficiency by supplying oxygen gas into gap, CIRP Annals—Manufacturing Technology, 40 (1991) 215–218.
11. Z.B. Yu, T. Jun, K. Masanori, Dry electrical discharge machining of cemented carbide. Journal of Materials Processing Technology, 149 (2004) 353–357.
12. Q.Y. Ming, L.Y. He, Powder-suspension dielectric fluid for EDM, Journal of Materials Processing Technology, 52 (1995) 44–54.
13. M.L. Jeswani, Electrical discharge machining in distilled water, Wear, 72 (1981) 81–88.

14. S. Abdulkareem, A.A. Khan, M. Konneh, Reducing electrode wear ratio using cryogenic cooling during electrical discharge machining, International Journal of Advance Manufacturing Technology, 45 (2009) 1146–1151.
15. Vineet Srivastava, Pulak M. Pandey, Effect of process parameters on the performances of EDM process with ultrasonic assisted cryogenically cooled electrode, Journal of Manufacturing Processes, 14 (2012) 393–402.
16. Vineet Srivastava (2012), Experimental Investigations and Analysis of Electrical Discharge Machining Using Ultrasonic Assisted Cryogenically Cooled Electrode, PhD diss., Indian Institute of Technology Delhi, India
17. J. N. Reddy, An introduction to the finite element method, Tata McGraw-Hill Publishing company Limited, New Delhi, 2005.
18. A. Erden, F. Arinc, M. Kogmen, Comparison of mathematical models for electric discharge machining, Journal of Material Processing and Manufacturing Science 4(1995) 163–176.
19. L. Li, Y.S. Wong, J.Y.H. Fuh, L. Lu, EDM performance of TiC-copper-based sintered electrodes, Materials and Design, 22 (2001) 669-678.
20. S. Abdulkareem, A. A. Khan, M. Konneh, Reducing electrode wear using cryogenic cooling during electrical discharge machining, Advanced Materials Research, Vols. 83-86 (2010) 672-679.
21. Vineet Srivastava, Pulak M. Pandey, Performance Evaluation of Electrical Discharge Machining (EDM) Process Using Cryogenically Cooled Electrode, Materials and Manufacturing Processes, 27(6) (2012) 683-688.
22. Vineet Srivastava, Pulak M. Pandey, Statistical modeling and material removal mechanism of electrical discharge machining process with cryogenically cooled electrode, Procedia Materials Science 5 (2014) 2004 – 2013.
23. D.D. Dibitonto, P.T. Eubank, M.R. Patel, A. Barrufet, Theoretical models of the electrical discharge machining process—I: a simple cathode erosion model, Journal of Applied Physics 66 (9) (1989) 4095–4103.
24. M.R. Patel, A. Barrufet, P.T. Eubank, D.D. DiBitonto, Theoretical models of the electrical discharge machining process—II: the anode erosion model, Journal of Applied Physics 66 (9) (1989) 4104–4111.
25. P.T. Eubank, M.R. Patel, M.A. Barrufet, B. Bozkurt, Theoretical models of the electrical discharge machining process. III. The variable mass, cylindrical plasma model. Journal of Applied Physics 73(11) (1993) 7900–7909.

26. A. Singh, A. Ghosh, A thermo-electric model of material removal during electric discharge machining, International Journal of Machine Tools & Manufacture 39 (1999) 669–682.
27. J. Marafona, J.A.G. Chousal, A finite element model of EDM based on the joule effect, International Journal of Machine Tools and Manufacture 46 (6) (2006) 592–602.
28. N. B. Salah, F. Ghanem, K.B. Atig, Numerical study of thermal aspects of electric discharge machining process, International Journal of Machine Tools & Manufacture 46 (2006) 908–911.
29. S.T. Jilani, P.C. Pandey, An analysis of surface erosion in electrical discharge machining, Wear 84(1983) 275-284.
30. S.N. Joshi, S.S. Pande, Thermo-physical modeling of die-sinking EDM process, Journal of Manufacturing Processes 12 (2010) 45-56.
31. S. N. Joshi, S. S. Pande, Development of an intelligent process model for EDM, International Journal of Advance Manufacturing Technology 45 (2009) 300–317.
32. Ranjeet Singh (2012). Modeling of vibratory EDM process, M.Tech. diss., Indian Institute of Technology Delhi, India
33. B. Izquierdo, J.A. Sanchez, S. Plaza, I. Pombo, N. Ortega, A numerical model of the EDM process considering the effect of multiple discharges, International Journal of Machine Tools and Manufacture 49 (2009) 220–229.

Appendix (A)

A.1 Program for the estimation of radius of crater

```
clc;

clear all;

close all;

hold on;

t=xlsread('C:\Users\Jashan Sharma\Desktop\gg.xlsx'); % gg is the excel file containing sorted nodes

x=t(:,2);

y=t(:,3);

z=t(:,4);

temp=t(:,5);

max1=max(temp);

len=length(temp)

k=1;

for i=1:1:len

  if z(i)==0 && y(i)==0

     if x(i)>=0

    x1(k)=x(i)

    t1(k)=temp(i)

     k=k+1;

     end

      end

end

figure(1)

plot(x1,t1,'r','LineWidth',1); hold on;
```

A.2 Program for the estimation of depth of crater

```
clc;

clear all;

close all;

hold on;

t=xlsread('C:\Users\Jashan Sharma\Desktop\gg.xlsx'); % gg is the excel file containing sorted nodes

x=t(:,2);

y=t(:,3);

z=t(:,4);

temp=t(:,5);

max1=max(temp);

len=length(temp)

k=1;

for i=1:1:len

  if x(i)==0 && y(i)==0

      if z(i)>=0

    z1(k)=z(i)

    t1(k)=temp(i)

     k=k+1;

     end

       end

end

figure(2)

plot(z1,t1,'r','LineWidth',2); hold on;
```

Thesis_Jashan.docx

ORIGINALITY REPORT

18%	14%	17%	%
SIMILARITY INDEX	INTERNET SOURCES	PUBLICATIONS	STUDENT PAPERS

PRIMARY SOURCES

1	S. N. Joshi. "Development of an intelligent process model for EDM", The International Journal of Advanced Manufacturing Technology, 03/14/2009 Publication	2%
2	researchinventy.com Internet Source	2%
3	www.linknovate.com Internet Source	1%
4	Das, S.. "EDM simulation: finite element-based calculation of deformation, microstructure and residual stresses", Journal of Materials Processing Tech., 20031125 Publication	1%
5	XIE, B.c.. "Numerical simulation of titanium alloy machining in electric discharge machining process", Transactions of Nonferrous Metals Society of China, 201108 Publication	1%

Srivastava, V., and P. M. Pandey.